Using Transit Vehicles as Probes to Monitor Community Air Quality and Exposure

Center for Transportation, Environment, and Community Health
Final Report

by

Mayra C. Chavez, Evan Williams, Ruey Long Cheu, Wen-Whai Li

June 30, 2021

DISCLAIMER

The contents of this report reflect the views of the authors, who are responsible for the facts and the accuracy of the information presented herein. This document is disseminated in the interest of information exchange. The report is funded, partially or entirely, by a grant from the U.S. Department of Transportation's University Transportation Centers Program. However, the U.S. Government assumes no liability for the contents or use thereof.

TECHNICAL REPORT STANDARD TITLE PAGE

1. Report No.	2.Government Accession No.	3. Recipient's Catalog No.
4. Title and Subtitle Using Transit Vehicles as Probes to Monitor Community Air Quality and Exposure		5. Report Date June 30, 2021
		6. Performing Organization Code
7. Author(s) Mayra C. Chavez Ph.D.(ORCID: 0000-0003-2511-0823) Evan Williams (ORCID: 0000-0002-3384-7836) Ruey Long Cheu Ph.D., P.E.(ORCID: 0000-0002-0791-2972) Wen-Whai Li, Ph.D., P.E.(ORCID: 0000-0003-1081-1889)		8. Performing Organization Report No.
9. Performing Organization Name and Address Department of Civil Engineering The University of Texas at El Paso 500 W. University Avenue El Paso, Texas 79968		10. Work Unit No.
		11. Contract or Grant No. 69A3551747119
12. Sponsoring Agency Name and Address U.S. Department of Transportation 1200 New Jersey Avenue, SE Washington, DC 20590		13. Type of Report and Period Covered Final Report 10/01/2019 - 06/30/2021
		14. Sponsoring Agency Code US-DOT

15. Supplementary Notes

16. Abstract

This project evaluates the feasibility of using transit vehicles traveling on fixed routes in a well-controlled residential community in El Paso for near-road exposure assessment. Continuous on-road measurements of four pollutants ($PM_{2.5}$, PM_{10}, NO_2, and O_3) were recorded using U.S. EPA FEM-designated monitors in conjunction with a GPS device for coordinates and vehicle speed. Concurrent near-road measurements of the same air pollutants at two near-road stationary sites were used to develop relationships with the mobile data. It was found that pollutant concentrations measured by mobile air monitors agree well with that collected at stationary sites. On-road $PM_{2.5}$ and PM_{10} concentrations closely resemble that measured at stationary sites. O_3 concentration was found to be ubiquitous in the community whether it's on-road, near-road, or in the community. On-road measurements of NO_2 showed slightly higher values compared to near-road sites. Furthermore, concentrations of transportation related air pollutants at traffic intersections in an environment with less traffic and topological features were found to be indistinguishable from that measured on road segments away from the traffic intersections. This study demonstrates that mobile air monitoring in a less traveled community can accurately detect the exposure concentrations that are representative of the community and near-road receptors. Further research should focus on how the mobile data can be used in exposure and health assessment and how the technique can be applied to characterize exposure concentrations at locations that stationary monitoring is not allowed or possible.

17. Key Words	18. Distribution Statement
Traffic Emissions, $PM_{2.5}$, PM_{10} NO_2, O_3, Air Modeling, Air monitoring	Public Access

19. Security Classif (of this report)	20. Security Classif. (Of this page)	21. No of Pages	22. Price
Unclassified	Unclassified		

Form DOT F 1700.7 (8-69)

Table of Contents

LIST OF TABLES

LIST OF FIGURES

CHAPTER 1: INTRODUCTION

Urban air pollution is a complex phenomenon in which pollutant concentrations vary spatially and temporally depending on the locations and strengths of emission sources, chemical and photochemical reactions of pollutants in the atmosphere, micro and macro meteorology of the region, topologic features of the environment, and regional-scale background concentrations prevailing in the region. Pollutants emitted from transportation related activities, particularly emissions associated with internal combustion engines, consist of a slew of hazardous air pollutants which pose significant adverse health effects to the population. Exposure to these transportation related air pollutants (TRAPs) could be harmful to human health and the environment. People who engage in outdoor physical activity in a polluted environment are likely to have increased health risks compared to those who have a more sedentary lifestyle, which may be counterproductive to the promotion of physical activity, although the benefits of physical activity outweigh the increased adverse health effects due to airway exposure to the TRAPs [1]–[4]. Different population groups, such as children, elderlies, pregnant women, or people living in near-road communities are especially susceptive to the TRAPs as reported in a number of epidemiological studies [5], [6].

Emerging evidence suggests that living in close proximity to traffic is particularly harmful to children. Approximately 3.2 million students attended schools located within 100 meters of a major roadway and an additional 3.2 million students attended schools located 100-250 meters from major roadways, as reported by Kingsley and his colleagues [7]. Schoolchildren living near busy highways had increased arterial stiffness [8], increased carotid intima-media thickness [9], decreased academic performance [10], increased absenteeism [11], increased clinical asthma symptoms [12], respiratory health [13]–[15], behavioral problems [16], and physical problems [17].

1.1 Background and Motivation

It is thus apparent that an accurate characterization of the spatio-temporal variation of urban air pollution would provide effective pollution control measures to reduce exposure and the subsequent adverse health effects for the public. Characterization of TRAPs, unfortunately, requires extensive air pollution monitoring and a speciation network that is costly, laborious, and

time-consuming; yet the results are never sufficient for conducting an impact assessment in a large study domain. To compensate the shortcoming of insufficient stationary monitoring locations, on-road monitoring of air pollution has been adopted to provide continuous spatial records of pollutant concentrations using equipment installed on various mobile vehicles such as cars, bicycles, or pedestrians.

Yu et al characterize the spatial and temporal variation of four TRAPs (BC, Particulate matter less than 2.5 micrometers in diameter ($PM_{2.5}$), PNC, and CO) in an urban community by taking 5-minute averages of pollutant concentrations collected by pedestrian walking on designated routes[18]. Each reported concentration in this study represents approximately a spatial average of 1,700 ft, based on an average adult walking speed of 4 miles per hour. Yu et al concluded that the spatio-temporal characteristics of the collected TRAP concentrations were consistent with findings in previously reported studies. Another mobile monitoring campaign was conducted in Montreal, Canada to evaluate the health effects of transportation emissions [19]. Mobile measurements of O_3 and NO_2 were carried out by walking and bicycling. They discovered that O_3 and NO_2 concentrations measured by the mobile sensors were consistent with the data reported by the city using refined, regulatory compliant instruments and that the diurnal variations of the two pollutants were consistent with the expected diurnal patterns in the city. Similar techniques were applied by strapping low-cost sensors on the wrist of an operator for mobile CO and NO_2 measurements in a near road air pollution study [20]. However, they reported low confidence in low-cost sensors and advocated developing data processing firmware for citizen science low-cost air monitoring.

PM sensors were installed on trash-trucks along garbage collection routes for air pollution measurements in Boston, MA [21]. It was noticed that a trash truck stops with engine on but off when the truck is at a halt. As a result, cross contamination due to its own tailpipe emissions of the truck might have introduced bias to the data collected. In addition, temporal variability of the PM concentration was limited by the operational hours of the garbage collection schedule. In another study, taxis were used as the vehicle for mobile monitoring by installing laser PM sensors

on fifty taxis to map PM pollution in a city [22]. The study concluded that the mobile measurements provide comparable data to that reported from fixed monitoring stations and suggested the use of mobile monitoring system for providing exposure concentrations in assessing public health risks and developing air pollution control policies.

The rapidly evolving mobile air monitoring technique has gained a strong foothold in air quality monitoring due to its unique nature of instantaneous temporal and spatial measurement. Nevertheless, some inherited challenges remain to be resolved, primarily in the relationship between its measurements and the conventional time-averaged air quality data typically collected at fixed stations. First, spatial resolution associated with mobile measurement is a major concern in mobile sampling. Whether a sample represents an average concentration over a long road segment, or a point measurement spaced apart by a given distance needs to be addressed. Furthermore, the length of the road segment or the distance between two sampling points (spatial resolution) depends strongly on the vehicle speed and idle time. For instance, Shi et al suggested an optimal spatial aggregation of 300 m based on their study in Hong Kong [23]. Second, the representativeness of a point measurement in space and time remains undefined. A point measurement collected along a long segment of a roadway could only represent an instantaneous observation of a three-dimensional concentration dataset that varies in space (1st and 2nd dimension) and time (3rd dimension). Third, TRAPs decrease rapidly from highway to near-road locations. Karner et al analyzed 41 roadside monitoring studies between 1978 and 2008 and concluded that almost all pollutants decay to background levels at a distance 115 m to 570 m from the edge of the road and the decay rate varies from one pollutant to another [24]. Venkatram et al showed that the concentration of an inert pollutant decays rapidly to less than 1/5 of its initial strength in 100 m in the direction normal to the roadway [25]. Recently, Cahill et al showed the downwind PM could be essentially undiluted at distances well beyond 200 m due to many uncontrollable factors, such as the existence of sound walls for at-grade freeways, elevated or filled section of a freeway, canopy vegetation, and classification of atmospheric stability condition [26].

Thus, it is of paramount importance to understand the relationship between the data collected using the mobile technique and that reported from a nearby fixed station.

1.2 Research Objectives

This project provides evidence for estimating near-road concentrations using transit vehicles traveling on fixed routes. Continuous on-road measurements of four pollutants ($PM_{2.5}$, $PM_{10,}$ NO_2, and O_3,) were recorded in conjunction with GPS locations. Concurrent near-road measurements were used to verify and provide associations with the on-road data. The study tests two hypotheses: 1) Community exposures to transportation pollutants can be represented by short-term spatio-temporal measurements using on-road air monitors; and 2) near-road receptors are not affected by the traffic emissions from surface street emissions and can be represented by on-road air monitors. The objectives of this study are to 1) provide reliable exposure concentration estimates for a community using transit vehicles equipped with mobile air monitors, and 2) evaluate associations of short-term TRAP concentrations with hourly exposure concentrations for near-road communities.

CHAPTER 2: METHODOLOGY AND STUDY DESIGN

We conducted a pilot-scale investigation to test the study design and hypotheses in a well-controlled residential community in El Paso. The study design could be extended in the future to any community located near a busy interstate highway. The implementation of this project provides a cost and time effective method for estimating the burden of traffic pollution on near-road community's health. Three tasks were implemented in this study including:

Task 1: Instrumentation Setup and Route Selection

We identified a bus route in the selected community and equipped a vehicle with three types of air monitors for $PM_{2.5}$, $PM_{10,}$ NO_2, and O_3 monitoring. All instruments were calibrated against the data recorded at the nearby state-operated air monitoring station.

Task 2: Air pollution measurements

On-road TRAP measurements were conducted using the transit vehicle equipped with the air monitors in conjunction with concurrent near-road measurements at two selected locations along the route.

Task 3: Traffic measurement and emission modeling

Traffic counts were conducted at 3 locations along the vehicle route using traffic counters concurrently to the air monitoring campaign. The traffic data were integrated into the MOVES emissions model to quantify vehicle emissions from different segments of the route.

Task 4: Data processing and Report preparation

The on-road data were processed along with the GPS data for generating concentration surfaces. The on-road data were compared to data collected at the near-road sites. Statistical analyses were conducted to examine the associations between the on-road and near-road TRAP data.

2.1 Study Design and Route Selection for Mobile Air Monitoring

This study was conducted in El Paso, Texas near the main campus of the University of Texas at El Paso (UTEP). Prior to the monitoring campaign all air quality sensors were calibrated against data collected by using U.S. EPA FRM-designated instruments at a state-operated air monitoring site, the CAMS 12 site. The UTEP air quality mobile station (based on a Chrysler cargo van) was modified to house the instruments with an external air inlet on top of the roof (Figure 1). The inlet was positioned approximately 2 ft above the top of the van to avoid the upwind turbulent

cavity zone formed on the roof while vehicle is moving and to minimize possible cross contamination of tailpipe emissions while vehicle comes to a halt. The routes for our mobile air monitoring are shown in Figure 1.

Figure 1 Air Quality Mobile Station

Mobile monitoring was conducted along two designated routes around the UTEP campus shown in Figure 2, with UTEP researchers driving at a speed of less than 30 miles per hour. The inner loop stays closer to the UTEP campus, going from Sun Bowl Drive to Oregon Street and then onto Schuster Avenue. The outer loop is very similar to the inner route, except that it bypasses Oregon Street and stays on Sun Bowl Drive longer so that it may go onto the busier Mesa Street. From Mesa Street, it turns back onto Schuster Avenue and follows the same path as the inner loop. In both routes, a detour is made on Schuster Avenue to take the mobile monitoring station closer to the CAMS 12 site, which is located approximately 50 ft off Rim Road, so that a comparison

could be made between the air pollutant data collected by the mobile monitoring station's instruments and CAMS 12 FRM data. In addition, a fixed site with the same air quality monitoring instruments was installed on Sun Bowl Drive to provide another location for data comparison. Both locations are shown in Figure 2. The routes were designed to cover an arterial road (Mesa Street) with multiple traffic lights, a low traffic surface street (Oregon Street), and streets of different traffic intensity. The total length of the large loop is approximately 10 miles, 8 miles for the smaller loop. Also shown in Figure 2 are the tube counter locations for counting arterial traffic on the route.

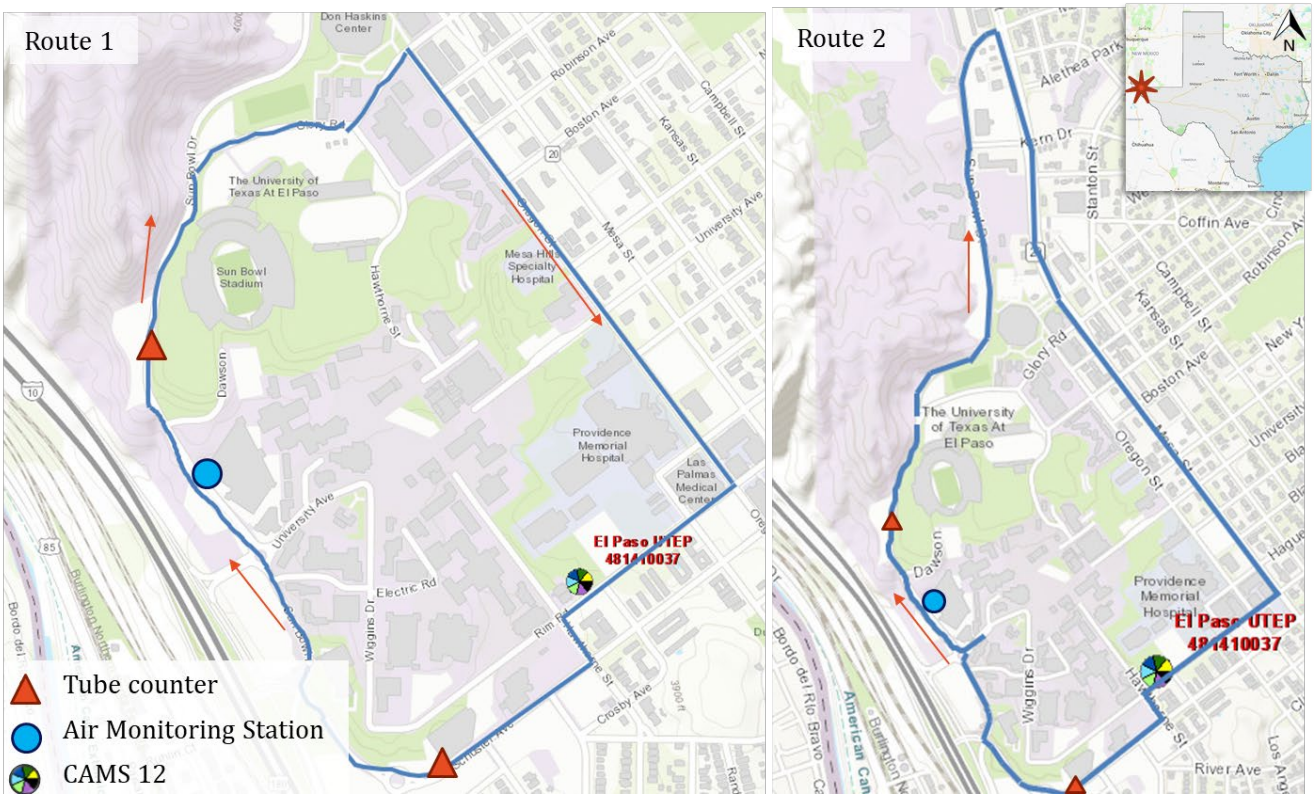

Figure 2 Study Area and Mobile Monitoring Routes

Each trip lasted about 12-15 minutes including stop-and-go at all traffic intersections. The air monitoring campaign began on November 10 and ended on November 20, 2020, for a period of 10 days. A total of 282 trips (170 outer loops and 112 inner loops) were conducted during this field study period resulting in around 60 hours of simultaneous collected, validated data of $PM_{2.5}$, PM_{10} O_3, NO_2, time, and GPS information. Table 1 summarizes the number of inner and outer loops driven during the on-road monitoring as well as the total number of hours of pollutant data collected.

Table 1 Number of Loops and Hours Driven

	10-Nov	11-Nov	12-Nov	13-Nov	14-Nov	16-Nov	17-Nov	18-Nov	19-Nov	20-Nov	Total
Inner Loop	4	8	12	12	12	12	12	12	16	12	**112**
Outer Loop	6	14	18	18	18	18	18	18	24	18	**170**
Hours Driven	3	5	7	6	6	6	6	6	7	6	**58**

2.2 Traffic Data Collection

2.2.1 Instrumentation and Setup

Traffic data were collected at two points along the route, one on Sun Bowl drive and another on Schuster Avenue. Their locations in the route can be seen in Figure 2. The TRAX Apollyon Counter/Classifier (JAMAR Technologies 2010) collected vehicle volume counts. Each counter included two tubes placed two feet apart; this method provides volume data and vehicle speed data for a two-way street. The vehicle volume was recorded for each hour of the day. Figure 3 shows the setup for the traffic data collection.

a) TRAX tube counter b) tubes laid on street c) students installing tube counter

Figure 3 Tube Counters for Traffic Collection

2.2.2 Data Collection

The tube counter categorizes each vehicle that passes it into different classes, those being bikes, cars and trailers, busses, and for vehicles larger than these by the number of axels they have. In order to utilize this set of data to develop emission estimates from the streets, vehicle class

fractions are needed for this study. The vehicle class fractions for the State of Texas were obtained from state vehicle class distributions provided by the Texas A&M Transportation Institute (TTI) for their previous work with the El Paso MPO on the Travel Demand Model (TDM) analysis (EP MPO 2013). These classes are not the same as the ones the tube counter categorizes vehicles into, and they must be translated into similar classes. The data collection period for the traffic counter was concurrent with the mobile monitoring campaign, November 10th, 2020, to November 20th, 2020.

2.3 Air Quality Data Collection

2.3.1 Instrumentation and Setup

Air quality data were collected by three different monitoring instruments. NO_2 was measured using 2B Technologies NO_2/NO/NOx Monitor TM [27]. O_3 was measured using 2B Technologies Model 202 O_3 Monitor [28]. Particulate matter was measured using GRIMM Portable Laser Aerosol spectrometer and Dust Monitor [29]. All three instruments are U.S. EPA FEM-designated air monitors.

2.3.2 Instrumentation Calibration

Prior to any field measurement, instruments were calibrated against pollutant data collected at the TCEQ-operated CAMS 12 site using FRM designated instruments. The monitors were placed in the UTEP field laboratory, a fenced area with a trailer equipped with electricity and is immediately adjacent to CAMS 12. All instruments were placed within 20 ft from their respective FRM devices for a side-by-side comparison, as shown in Figure 4.

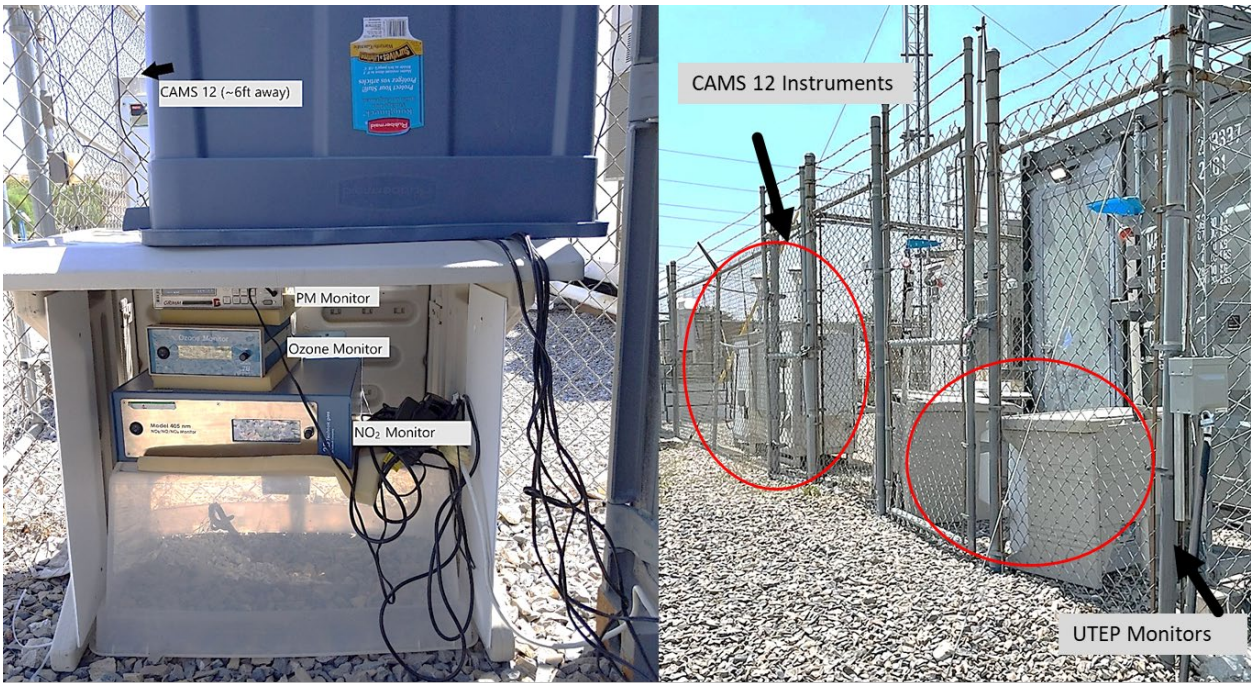

a) Monitors used in UTEP study b) zoomed-out view showing CAMS 12 instruments 6 ft away

Figure 4 Calibration Set-Up of Monitoring Instruments

Pre-calibration was performed for two weeks before the study period, and one week for post-calibration immediately after the field study. Post-calibration could not be completed for NO_2 data because FRM data were not collected at CAMS 12 during the period. Correlation plots and times series data for each pollutant and monitor are documented in Appendix A. Summarized in Table 2 are the pre- and post-calibration data displaying consistent performance of the instrument with negligible electronic drift. The final calibration equation for each monitor was developed using the whole set of calibration data (both pre- and post-calibration data). Table 2 also displays the final calibration equation and associated R^2-value used for data processing.

Table 2 Calibration Data

	Final Calibration		Pre-Calibration		Post-Calibration	
$PM_{2.5}$						
Monitor	On-road	Sun Bowl	On-road	Sun Bowl	On-Road	Sun Bowl
Equation	y = 0.63x+ 3.7674	NA[1]	y = 0.68x + 3.46	y = 2.72x+ 3.69	y = 0.53x + 4.14	NA[1]
R^2	0.7631		0.8872	0.8802	0.6013	
PM_{10}						
Monitor	On-road	Sun Bowl	On-Road	Sun Bowl	On-Road	Sun Bowl
Equation	y = 1.20x + 7.8273	NA[1]	y = 1.33x + 6.09	y = 2.36x + 13.73	y = 0.74x – 1.18	NA[1]
R^2	0.8082		0.8659	0.8849	0.7446	
NO_2						
Monitor	On-road	Sun Bowl	On-Road	Sun Bowl	On-Road	Sun Bowl
Equation	y = 0.38x + 10.33	y = 1.0x + 3.88	y = 0.38x+ 10.33	y = 1.0x+ 3.88	NA[2]	NA[2]
R^2	0.5112	0.9426	0.5112	0.9426		
O_3						
Monitor	On-road	Sun Bowl	On-Road	Sun Bowl	On-Road	Sun Bowl
Equation	y = 1.03x+ 1.02	y = 1.11x– 3.80	y = 1.06x – 0.23	y = 1.1x– 3.84	y = 1.0x+ 3.85	y = 1.13x– 3.96
R^2	0.966	0.9908	0.9882	0.9915	0.9667	0.9874

NA[1]: equipment malfunction during the study

NA[2]:FRM data not available for calibration during the post calibration period

2.3.3 Field Study

One set of instruments were installed inside the on-road mobile station driven on the routes. Monitors were placed on a shelving unit that helped minimize vibration of the instruments during mobile monitoring. This shelving unit also raised the height of the instruments, which allowed the inlet tubes of the monitors to reach outside via a pipe that went through the roof. Inlet tubes were also shielded from rainwater. The instrument set-up is shown in Figure 5 along with the GPS unit. NO_2 readings were collected every 10 seconds, O_3 every 5 seconds, and $PM_{2.5}$ and PM_{10} every 6 seconds. These intervals are the lowest allowed by each monitor. A Columbus P-1 Professional GPS Data Logger was also placed with the monitors, which collected longitude, latitude, and speed every second. At the start of every day, the monitors were turned on and allowed to run for 30 minutes before beginning the mobile monitoring route. This 30-minute wait period allowed the monitors internal temperatures to stabilize so that readings could be most accurate.

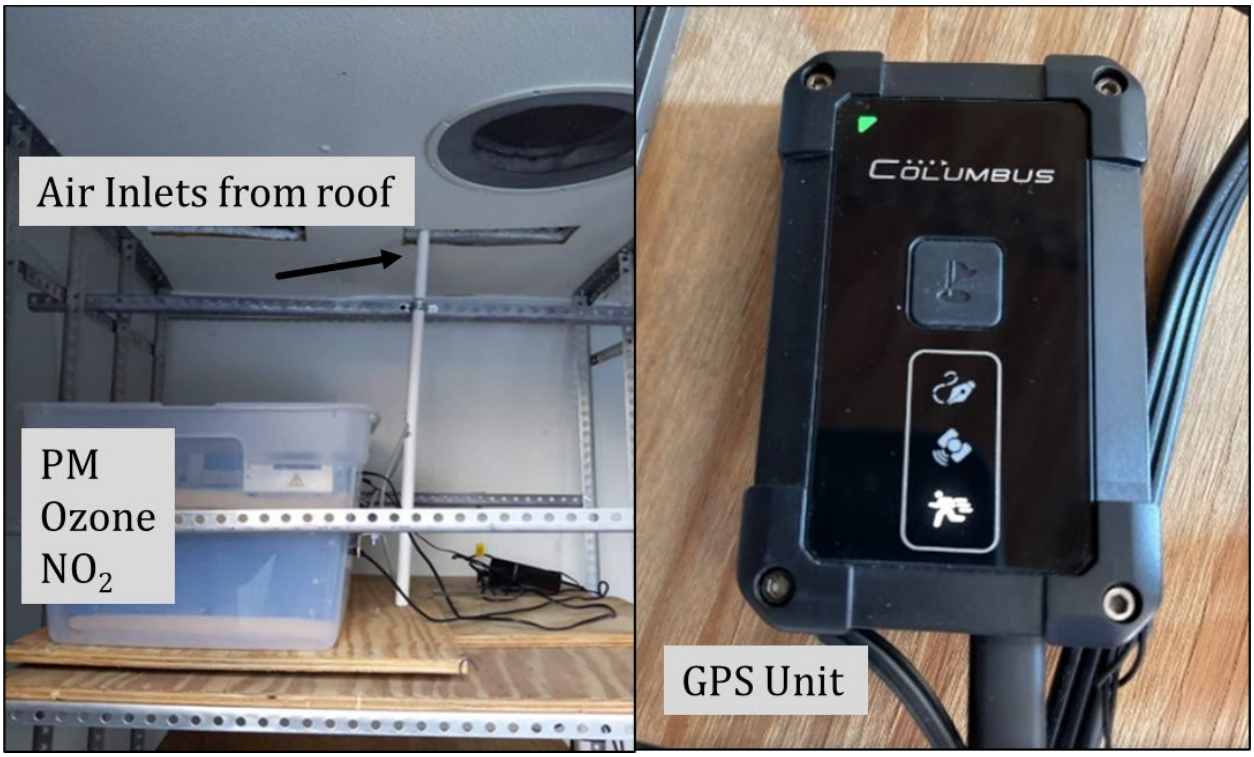

Figure 5 Instruments Inside Mobile Monitoring Station (Air Monitors And GPS)

Another set of the air monitoring instruments were placed inside an enclosure at the Sun Bowl site to collect stationary data 5 meters away from the road, shown in Figure 6. This set of instruments collected TRAP data every 5 minutes and ran for the entire collection period, day and night. The instruments were protected from rain and wind by a housing unit, which also provide shade for the instruments to maintain an adequate range of operating temperature. Unfortunately, the PM monitor at this station failed four days into the study period and could not be fixed or replaced before the end of the collection time.

Figure 6 Instruments at Sun Bowl Station and Location Relative to Road

2.3.4 Data Processing

As stated previously, each of the three monitors had a different lowest resolution for recording data points. In order to obtain synchronized data among the monitors and the GPS unit, the pollutant data were interpolated between two consecutive readings by assigning the ending reading to all 1-second data in the interval between the two readings. For example, the last data point recorded for $PM_{2.5}$ was used to represent each of the previous 6 seconds. This 1-second data were used to spatially plot pollutant concentrations and create averages in 25-m hexagonal bins. An example of the hexagonal bins is shown in Figure 7.

ArcGIS averages all data points within 25 meters and hexagonal bins were chosen to create a more even coverage of point aggregation compared to square areas. Data points provided by the GPS were slightly off from the base layer map due to the projection of the map in the ArcGIS software. The high number of 1-second data points over a daily period made visual analysis difficult and the hexagonal bins provide a more general view of the pollutant concentrations along the route.

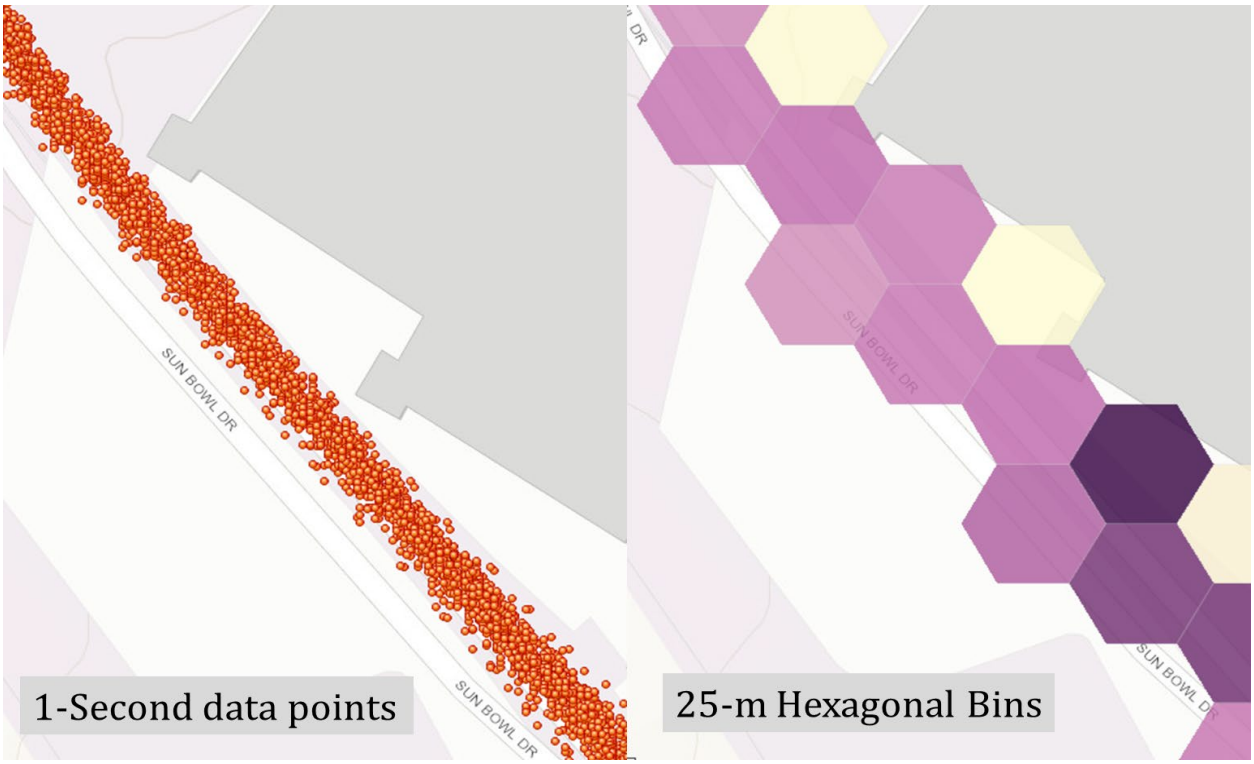

Figure 7 1-Second Data Points to Hexagonal Bins for Averaging

2.4 Emission Modeling

The traffic data generated from field traffic counts at two arterials were used to generate vehicle emissions factors and emissions inventory. The MOVES emission model was used to generate emissions estimates for these two roads in model domain. Temperature, humidity, vehicle speed, vehicle volume, and vehicle fleet mix information were all considered as variables in MOVES modeling. Each model run corresponds to one hour during each of the four weekday time periods (morning peak, midday, evening peak and overnight) for the month during the analysis. The four weekday time periods are:

- Morning peak emissions based on data 7 a.m. to 9 a.m.
- Midday emissions based on data from 10 a.m. to 3 p.m.
- Evening peak emissions based on data from 4 p.m. to 7 p.m.
- Overnight emissions based on data from 8 p.m. to 6 a.m.

A specific hour within each of the four time periods was modeled and the results were extrapolated to cover the entire day. Hourly tube counter data were processed to obtain hourly

averages over the two-week period for weekdays and weekend averages. The time span covered is the month of November and the distinct time periods are morning, midday, evening, and overnight. Emissions Factors (EFs) were calculated for a typical weekday, Saturday, and Sunday during the month. A total of 12 MOVES runs were conducted according to all the parameters of the study for each scenario. The speed range is from 20 mph to 30 mph based on posted speed limits in the two arterials.

The EFs produced by MOVES are in terms of grams/hour for each peak time period and included separate EFs for running exhaust emissions and brake wear and tire wear. Inventory emissions were also obtained for the two-road links.

CHAPTER 3: MODELING OF NEAR-ROAD POLLUTANT CONCENTRATIONS

This chapter discusses the process necessary in generating the EFs to be used in this study's analysis. The traffic data generated from field traffic counts at arterials were used to generate vehicle emissions rates. This was done with the EPA's Motor Vehicle Emissions Simulator (MOVES). The MOVES emission model was used to generate emissions estimates for two arterial roads, frequently traveled in the model domain. The latest version of the MOVES model is called MOVES3 and was released in March 2021 (EPA-420-R-21-004 March 2021).

3.1 MOVES Model Inputs

MOVES uses traffic and vehicle fleet data to calculate emissions rates or inventory values of pollutants. Figure 8 illustrates the flow of data during the MOVES modeling process including inputs needed.

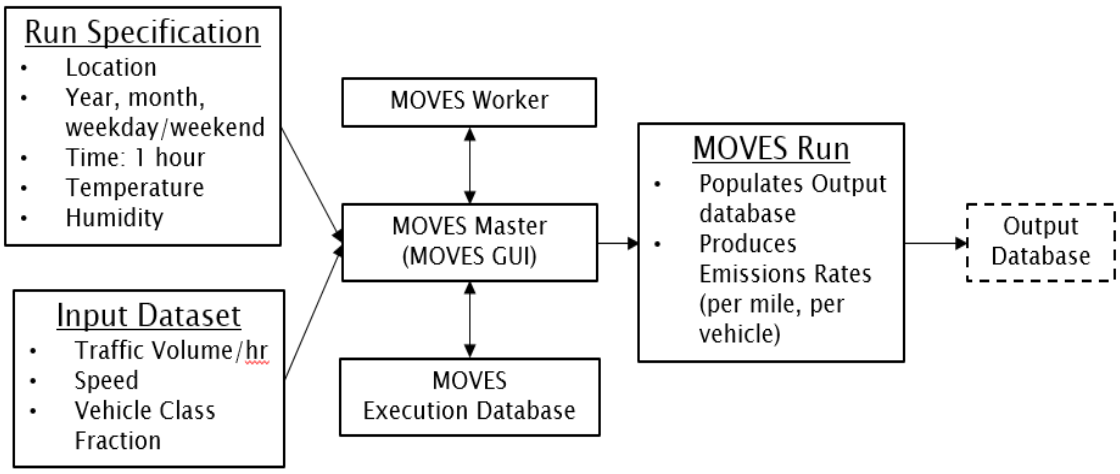

Figure 8 MOVES Model Data Flow

The MOVES model includes six road types: off-network, rural restricted, rural unrestricted, urban restricted, urban restricted. For the purpose of this emission estimation, arterials are classified as "urban restricted" roads. Emissions evaluation based on PM hot-spot process are based on the temporal attributes as required by the EPA hot-spot guidance [30]. Depending on the level of sophistication required for the activity data for a given project, the emission estimates to be generated may range from a daily average-hour and peak-hour value to hourly estimates for all days of the year. The emission factor generation framework in this study uses the peak-hour, or

average-hour traffic volume for a typical weekday during the following four daily peak periods, extracted from the observed traffic data in the two arterials:

- Morning peak emissions based on data 7 a.m. to 9 a.m.
- Midday emissions based on data from 10 a.m. to 4 p.m.
- Evening peak emissions based on data from 4 p.m. to 7 p.m.
- Overnight emissions based on data from 7 p.m. to 7 a.m.

A specific hour within each of the four time periods is modeled and the results are presented as total inventories for each of the representative hours. The average of the hours during each time period is modeled for four different hours in MOVES3.

3.2 $PM_{2.5}$ Emission Factor Generation for Study Area

A total of 8 MOVES3 runs were conducted according to all the parameters of the study. The time span covered is the month of November and the distinct time periods are morning, midday, evening, and overnight. Emissions inventories were calculated for a typical weekday and, typical weekend, during November 2020. All input data for MOVES3 can be set up in two main steps. The first step is setting up the RunSpec input parameters. The details of this study's RunSpec inputs are summarized in Table 3.

Table 3 MOVES3 RunSpec Inputs

Parameters	Specification for Run
Scale	Project-Level
Time Span	Nov 12-20 2020, Weekday, Weekend
Geographic Bounds	El Paso County
Vehicles/Equipment	Motorcycle, Passenger Car, Passenger Truck, Light Commercial Truck, Intercity Bus, Transit Bus, School Bus, Refuse Truck, Single Unit Short-haul Truck, Single Unit Long-haul Truck, Motor Home, Combination Short-haul Truck, Combination Long-haul Truck
Road Type	Urban Unrestricted
Pollutants and Processes	$PM_{2.5}$, PM_{10}. NO_2
Output	Inventory (grams/link)

The second step consists of preparing MOVES input data through the MOVES Project Data Manager (PDM) user interface. In general, there are two types of data required for project-level MOVES3 runs:

- Site-specific traffic information, including traffic volumes, and speed.

- Local-specific inputs, including regional-level vehicle age, source distribution, meteorology, fuel supply, and I/M program parameters.

The following sections detail the input values necessary for generating the pollutant inventories for the two major arterials in the study area using MOVES3.

3.2.1 Site-Specific Traffic Information

Traffic data were collected for 2 arterial roads in the study area during the study period in November 2020. The following section details how the traffic information for all the roadways in the study area was obtained. Figure 9 shows the length and orientation of the two links modeled with MOVES3.

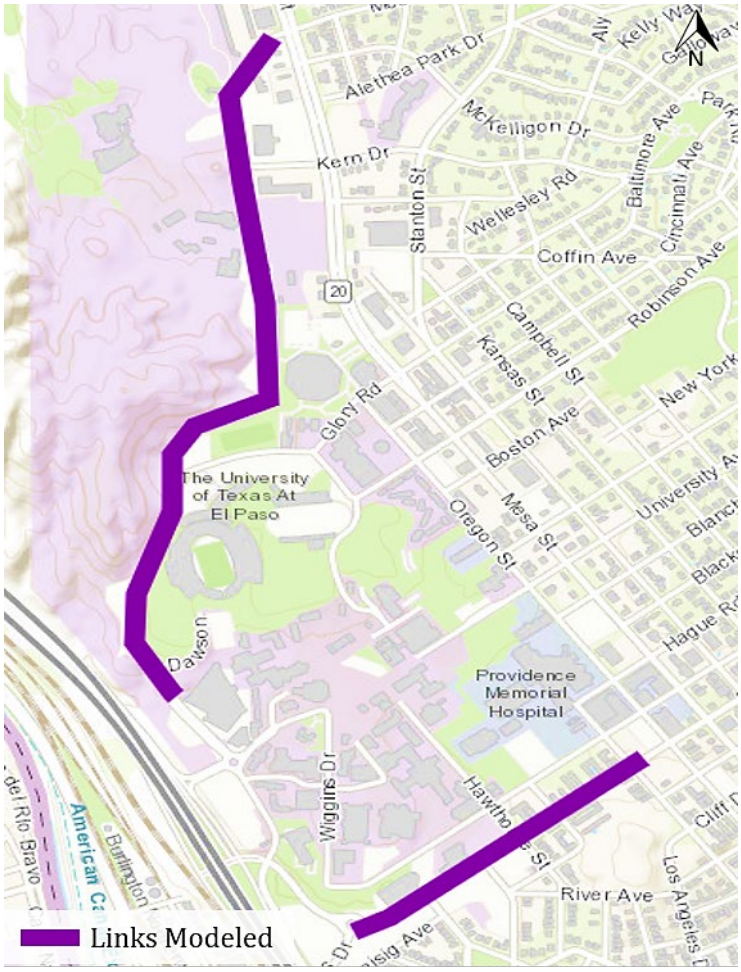

Figure 9 Links Modeled in MOVES3

3.2.2 Local-Specific Inputs

Local-specific inputs generally include regional-level vehicle age, source type distribution, fuel supply, and meteorology. The meteorology data, which consists of hourly temperature and humidity, was obtained from the UTEP CAMS 12 site which was chosen to represent the meteorology for the study area. The other local-specific inputs, pertaining to vehicle fleet information, were provided by the El Paso MPO [31].

CHAPTER 4: DATA PROCESSING AND RESULTS

4.1 Air Quality Data Visualization and Database Structure

On-road air quality data of 4 TRAPs and the GPS records were synchronized to have a common time resolution of 1 second. Figure 10 provides an illustration of the locations of $PM_{2.5}$ data collected from all runs in a typical road segment. Each dot in Figure 10 represents the location and magnitude of a $PM_{2.5}$ data point, recorded along with the GPS location and time of the day. The density of the data point in a road segment varies depending on the frequency of trip and the speed of the vehicle.

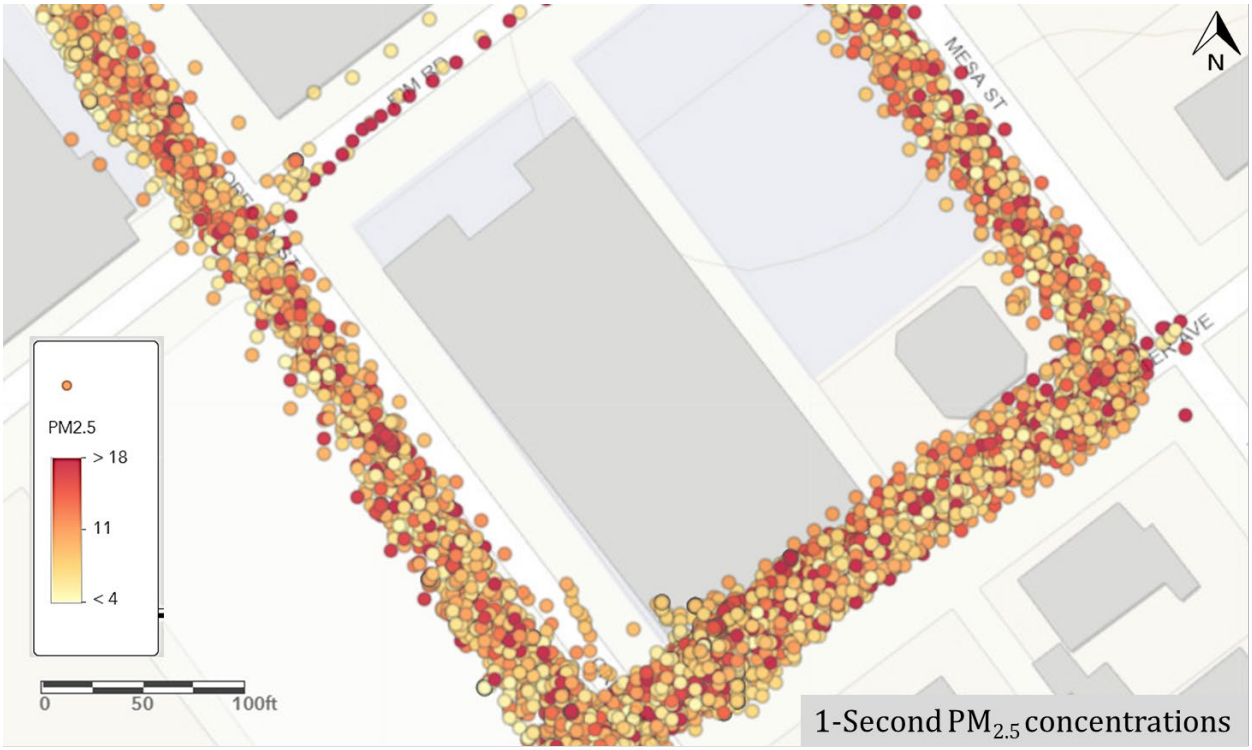

Figure 10 Road Segment Showing 1-Second $PM_{2.5}$

Once each pollutant was extrapolated to a 1-second resolution, a database was created for each day of the on-road monitoring campaign. This database was used in the spatial analysis done using ArcGIS as well as any statistical and data analysis using Jupyter Notebook (Python) and Excel.

The air pollution data collected during this study was processed for accuracy and completeness. Values reported by the monitors as negative, due to being below the monitors' method detection, were corrected. The reported concentrations can be negative due to zero drift in the electronic

instrument output, data logger channel, or calibration adjustments to the data. Slightly negative values were automatically set to 0.5 (i.e., 1/2 of the detection limit), unless the negative values were more than three consecutive values; these were considered missing data. The finalized air pollution data were also adjusted using the calibration equation for each instrument found from the pre- and post-calibration data.

This database example is outlined in bracketed sections in

Table 4. Once each pollutant was extrapolated to a 1-second resolution, a database was created for each day of the mobile monitoring campaign; an example of this database structure is shown in

Table 4. The interpolated concentrations by second for each pollutant are boxed in bold frame in the table according to the beginning and ending time of the data recorded by the respective monitor. All synchronized data are shown in the same row in Table 4 with the same coordinates and vehicle speed. This database was used in the spatial analysis done using ArcGIS as well as any statistical and data analysis using Jupyter Notebook (Python) and Excel. Since on-road monitoring was not able to be done for continuous hours each day, due to schedules of the researchers, some databases had blank sections for times off-line.

Table 4 Database Example for Nov 11

Date and Time	PM_{10}	$PM_{2.5}$	NO_2	O_3	Latitude	Longitude	Speed (mph)
11/12/2020 8:40:30	21.75	10.15	7.99	6.93	31.769	-106.505	23.5
11/12/2020 8:40:31	21.75	10.15	27.14	7.45	31.769	-106.505	23.4
11/12/2020 8:40:32	21.75	10.15	27.14	7.45	31.769	-106.505	22.4
11/12/2020 8:40:33	21.75	10.15	27.14	7.45	31.769	-106.505	20.9
11/12/2020 8:40:34	37.35	8.32	27.14	7.45	31.769	-106.505	19.9
11/12/2020 8:40:35	37.35	8.32	27.14	7.45	31.770	-106.505	19.1
11/12/2020 8:40:36	37.35	8.32	43.75	7.45	31.770	-106.505	17.5
11/12/2020 8:40:37	37.35	8.32	43.75	7.45	31.770	-106.505	16.5
11/12/2020 8:40:38	37.35	8.32	43.75	7.45	31.770	-106.505	16.3
11/12/2020 8:40:39	37.35	8.32	43.75	7.45	31.770	-106.505	16.5
11/12/2020 8:40:40	21.15	7.75	43.75	7.45	31.770	-106.505	16.4
11/12/2020 8:40:41	21.15	7.75	41.52	9.01	31.770	-106.505	14.5
11/12/2020 8:40:42	21.15	7.75	41.52	9.01	31.770	-106.505	13.3
11/12/2020 8:40:43	21.15	7.75	41.52	9.01	31.770	-106.505	13.1
11/12/2020 8:40:44	21.15	7.75	41.52	9.01	31.770	-106.505	12.6
11/12/2020 8:40:45	21.15	7.75	41.52	9.01	31.770	-106.506	12.7
11/12/2020 8:40:46	14.79	7.44	19.95	9.01	31.770	-106.506	12.7
11/12/2020 8:40:47	14.79	7.44	19.95	9.01	31.770	-106.506	13.9
11/12/2020 8:40:48	14.79	7.44	19.95	9.01	31.770	-106.506	15
11/12/2020 8:40:49	14.79	7.44	19.95	9.01	31.770	-106.506	16.1
11/12/2020 8:40:50	14.79	7.44	19.95	9.01	31.770	-106.506	17.1

4.2 Air Quality Data Results

4.2.1. Descriptive Statistics

Summary of the hourly pollutant concentration along all routes during the study period is presented in box plots in Figure 11 where the distribution of data for the hour are marked in terms minimum (Q1-1.5•IQR), first quartile (Q1), median, third quartile (Q3), and maximum (Q3+1.5•IQR).

Figure 11 also represents the spatio-temporal averages of the pollutant concentrations for the hour along the route covered by the vehicle. As expected, the diurnal variation of $PM_{2.5}$ concentration resembles closely to that of PM_{10} and the overall average of $PM_{2.5}$ concentration is approximately 30% of PM_{10}. After removing outliers, hourly PM_{10} peaks at 75 $\mu g/m^3$ in the evening around 6 pm as well as $PM_{2.5}$ at around 15 $\mu g/m^3$. A secondary PM peak around 12 pm is also observed in the figure. In El Paso, PM in general peaks in the early morning hours around 6 am and again in the early evening hours around 6 pm due to the traffic intensity [32]. The ratio for $PM_{2.5}$ to PM_{10} is around 0.25 [32], [33] due to the high fugitive emissions from geologic sources (surrounding desert) and traffic-enhanced emissions of road dust. On-road PM concentrations are

expected to be closely associated with traffic. In El Paso, as well as in many major cities, traffic intensifies in the early morning and late afternoon which coincides with the diurnal occurrences of PM peaks. During the time of this study, traffic patterns in the study domain, however, vary differently from the general pattern of morning and evening peaks due to the SARS-CoV2 pandemic.

NO_2 data in general show a steady increase and peaks in the evening. NO_2 is a primary pollutant from tailpipe emissions and a precursor in the O_3-NO_2 photolysis. NO_2 is rapidly depleted in the atmosphere during the day especially under strong solar radiation to form O_3. NO_2 begins to accumulate after sunset when the O_3-NO_2 photolysis ceases to function. In the meantime, O_3 begins to increase in the morning when the sun rises, peaks in the early afternoon when the solar radiation peaks and decreases to the minimum after the sunset. Figure 11c and d illustrate the O_3-NO_2 cycle for the Paso del Norte region. It also shows that NO_2 steadily increases from the morning, maintains at an equilibrium level throughout the day, and begins to peak in the late afternoon. The variation shows the balance between the recurring traffic emissions and NO_2 photolysis during the day. As is observed in later sections, O_3 measured by on-road monitoring is highly correlated with O_3 measured at any near-road site in the study area. This further exemplifies the homogenous distribution of O_3 in the region, as compared to the concurrent TCEQ O_3 data. Hourly boxplots for the pollutant data are shown for every day in Appendix B.

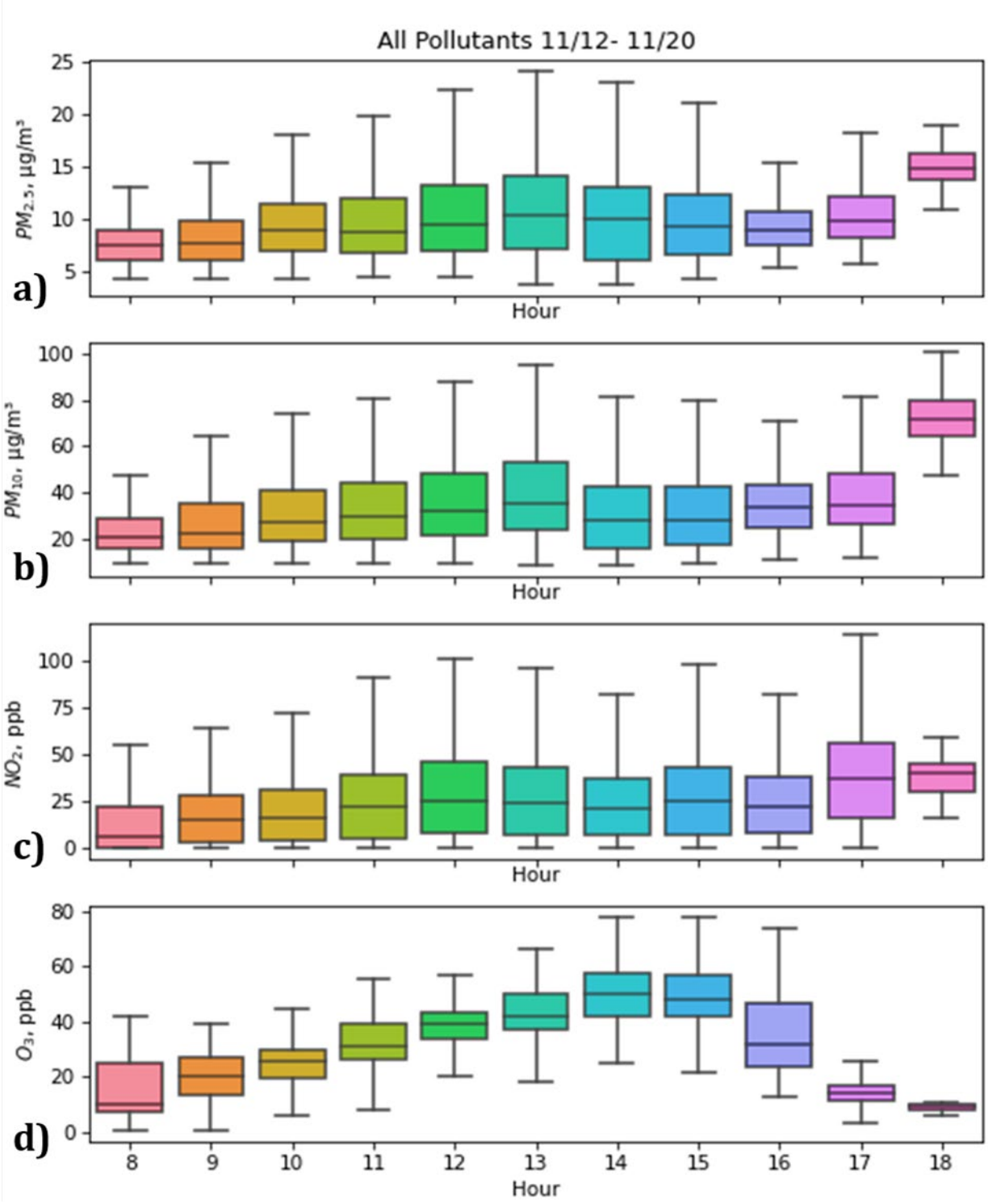

Figure 11 Hourly Boxplot: Pollutant data for all study period

4.2.2. Spatio-temporal averages of on-road concentrations

Figure 12 through Figure 19 show the time-averaged spatial distribution of all four pollutants as measured by the mobile monitoring route. Each of the four panels in a figure represents the averaging of all points for a specific pollutant for that day when data were collected (from 2 to 8 hours) that are within the 25-m hexagons discussed previously. The figures include the monitoring data during the study starting on November 12th to November 20th. It can be seen that although PM values differ from day to day, they appear at high concentrations in the same locations on the route, along Mesa Street and on Sun Bowl Drive as it meets the Mesa intersection. PM also shows higher values along parts of the route with more intersections, whether free-flowing or stop-and-go. NO_2 values seem to peak at intersections and stops on the mobile monitoring route. O_3 actually follows a similar patter peaking at slower parts of the route and at stops and intersections, although in general, this pollutant is the most ubiquitous on the mobile monitoring route.

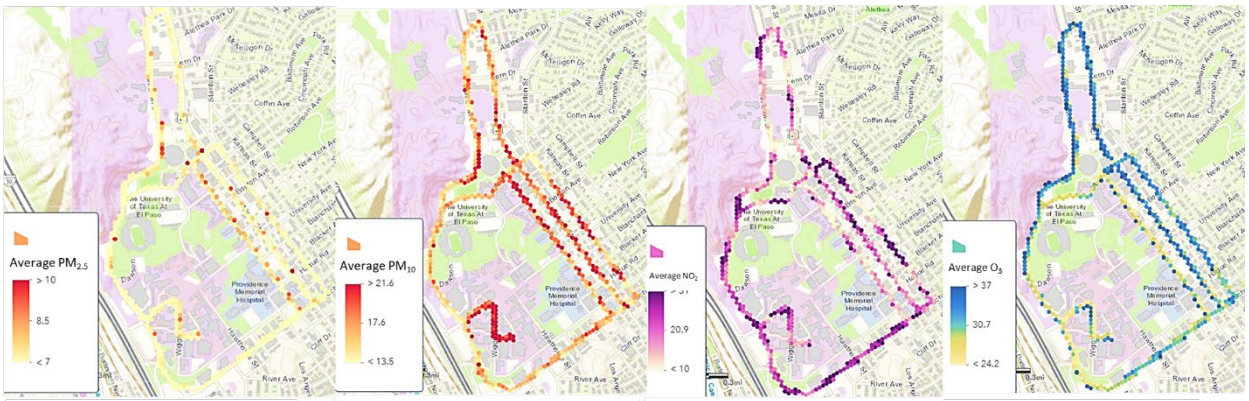

Figure 12 Daily Average of On-Road Concentrations (Nov 12)

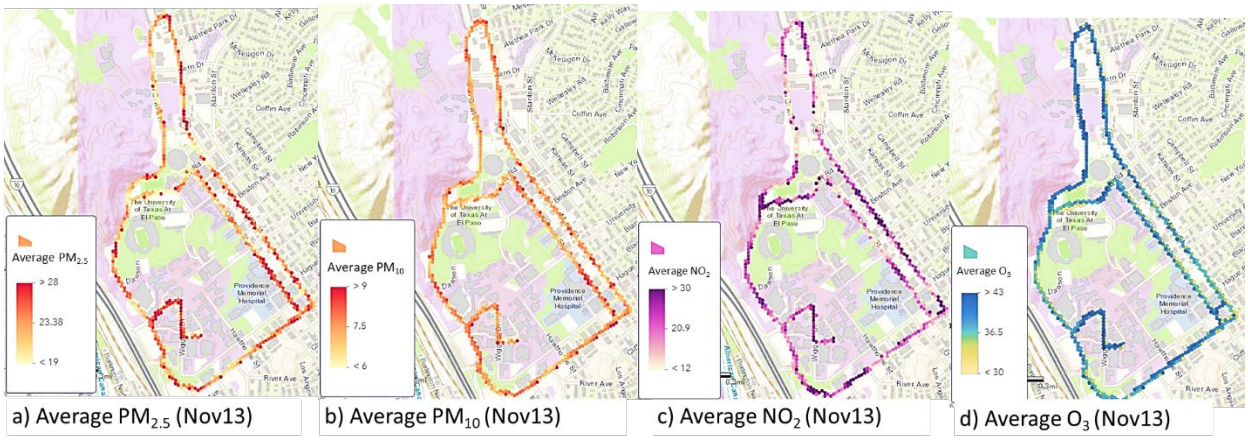

Figure 13 Daily Average of On-Road Concentrations (Nov 13)

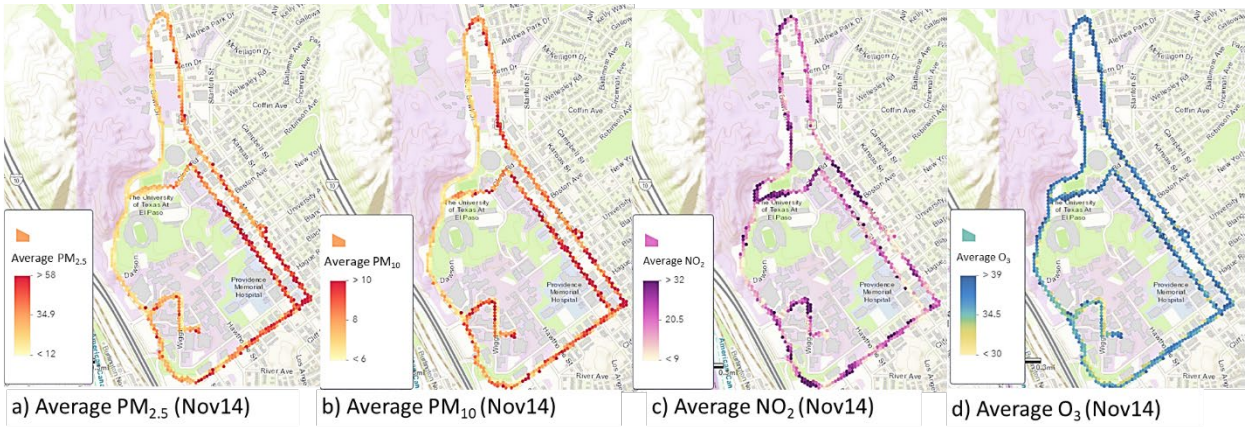

Figure 14 Daily Average of On-Road Concentrations (Nov 14)

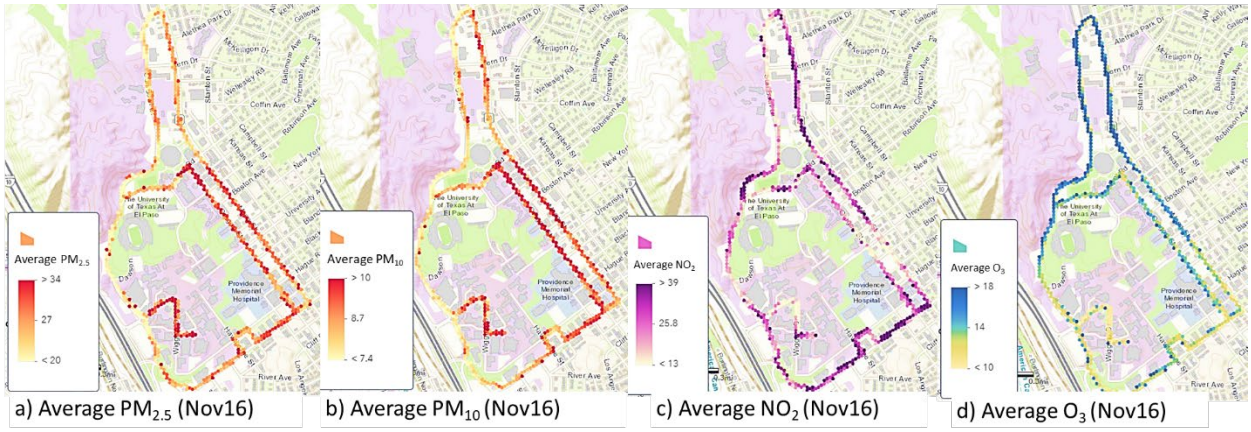

Figure 15 Daily Average of On-Road Concentrations (Nov 16)

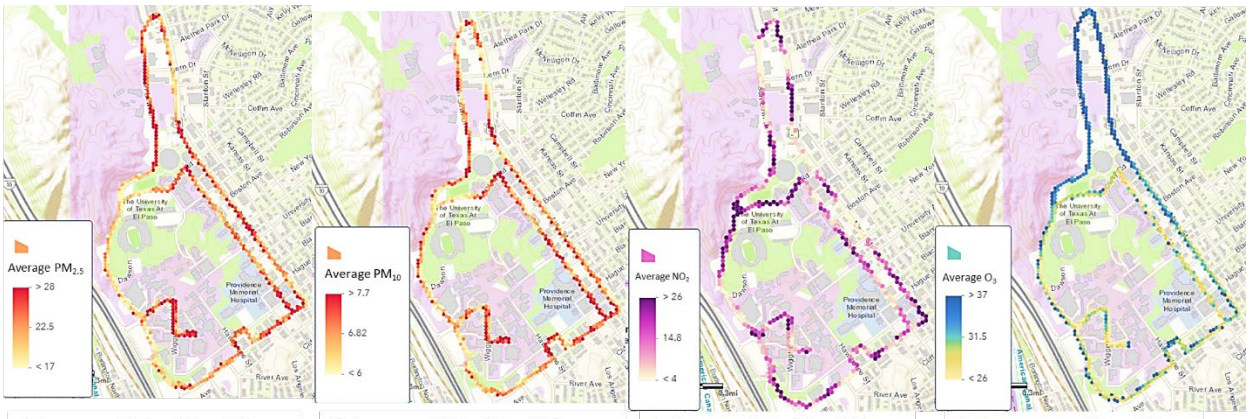

a) Average $PM_{2.5}$ (Nov17) b) Average PM_{10} (Nov17) c) Average NO_2 (Nov17) d) Average O_3 (Nov17)

Figure 16 Daily Average of On-Road Concentrations (Nov 17)

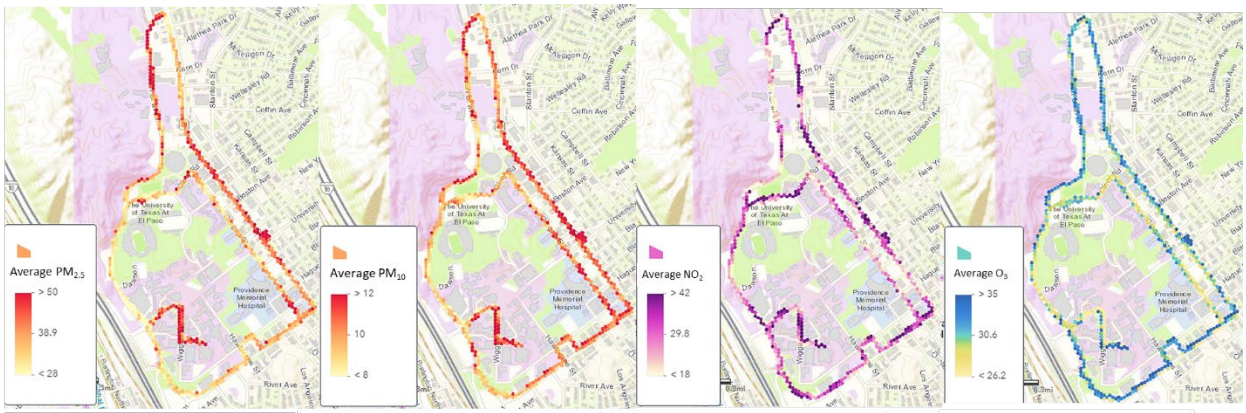

a) Average $PM_{2.5}$ (Nov18) b) Average PM_{10} (Nov18) c) Average NO_2 (Nov18) d) Average O_3 (Nov18)

Figure 17 Daily Average of On-Road Concentrations (Nov 18)

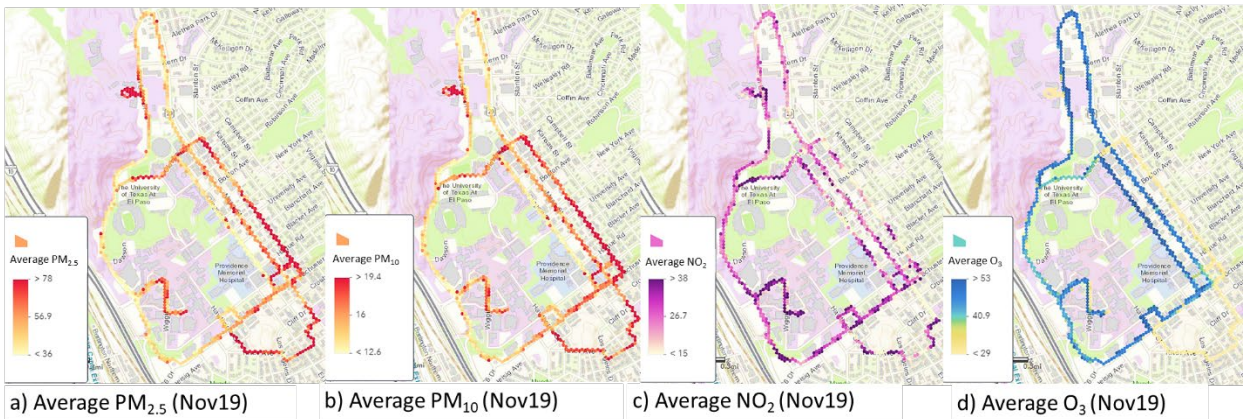

a) Average $PM_{2.5}$ (Nov19) b) Average PM_{10} (Nov19) c) Average NO_2 (Nov19) d) Average O_3 (Nov19)

Figure 18 **Daily Average of On-Road Concentrations (Nov 19)**

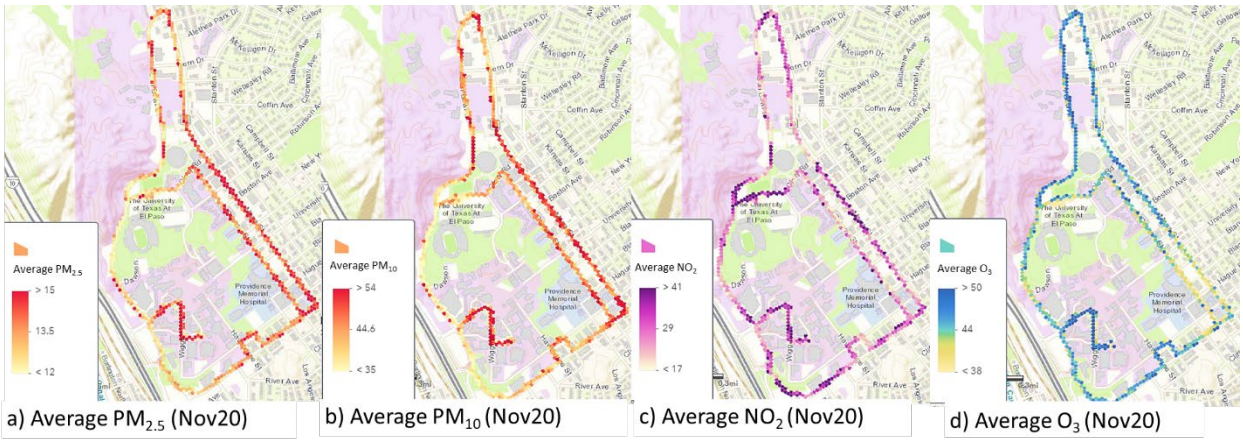

Figure 19 Daily Average of On-Road Concentrations (Nov 20)

Figure 20 shows the averaging of all pollutant values within 25-m hexagonal areas averaged over all the days of the study. This visualization helps show hotspots at different locations in the study in a more generalized term over the 10 days. PM shows higher values along parts of the route with more intersections, whether free-flowing or stop-and-go. NO_2 values seem to peak at intersections and stops on the on-road monitoring route. O_3 follows a similar pattern peaking at slower parts of the route and at stops and intersections, although in general, this pollutant is the most ubiquitous on the on-road monitoring route. It can be seen that in the 10-day period as well as in similar daily maps, PM_{10} appears highest at the most congested arterial, Mesa Street, in the northwest part of the route. $PM_{2.5}$ peaks at these locations as well. NO_2 peak values for the 10-day period are clustered and evident especially at the two roundabout locations on the on-road monitoring route. This increase in NO_2 may be attributed to the stop and acceleration of vehicles as they drive through the roundabout. As seen in the daily maps, O_3 had a more uniform distribution on the on-road monitoring route, showing slightly higher values where the vehicle was operating at higher speeds, in the stretch of Sun Bowl as it approaches the Mesa intersection. It is also of note that NO_2 and O_3 appeared to peak at opposite levels. Areas along the on-road monitoring route that have higher levels of NO_2, coincide with areas where O_3 is slightly lowest.

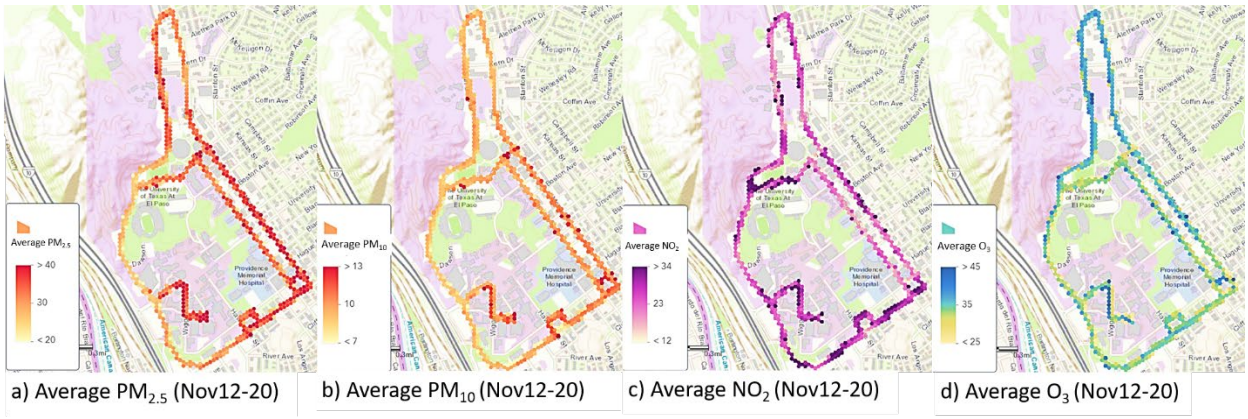

a) Average $PM_{2.5}$ (Nov12-20) b) Average PM_{10} (Nov12-20) c) Average NO_2 (Nov12-20) d) Average O_3 (Nov12-20)

Figure 20 All Period Average of On-Road Concentrations

4.2.3 Intersection Analysis

Traffic intersections at busy streets have been identified as hot spots for transportation air pollution. A detailed assessment of air pollution at traffic intersections was performed by evaluating pollutant data at a traffic intersection. We compared the concentration at an intersection to the on-road concentrations away from the intersection (50 meters off an intersection in either direction). The concentration at an intersection was calculated from the average of all on-road concentrations with a 50 m diameter zone center at the intersection. Figure 21 shows the zones before, after, and in the intersection used in one of the intersection analyses. Three intersections were selected for the analysis from the collected data. These intersections are Mesa and Sun Bowl, Mesa and University, and Mesa and Schuster. This analysis was also done with 25-m diameter zones, shown in the figure with dashed circles. The pollutant data were extracted from these zones and then hourly averaged and plotted on a time series graph for comparison. The goal of this analysis is to compare the before, in, and after air pollutant values for each pollutant and to understand if there are any trends, such as tendency to have higher values in the intersection as opposed to before and after.

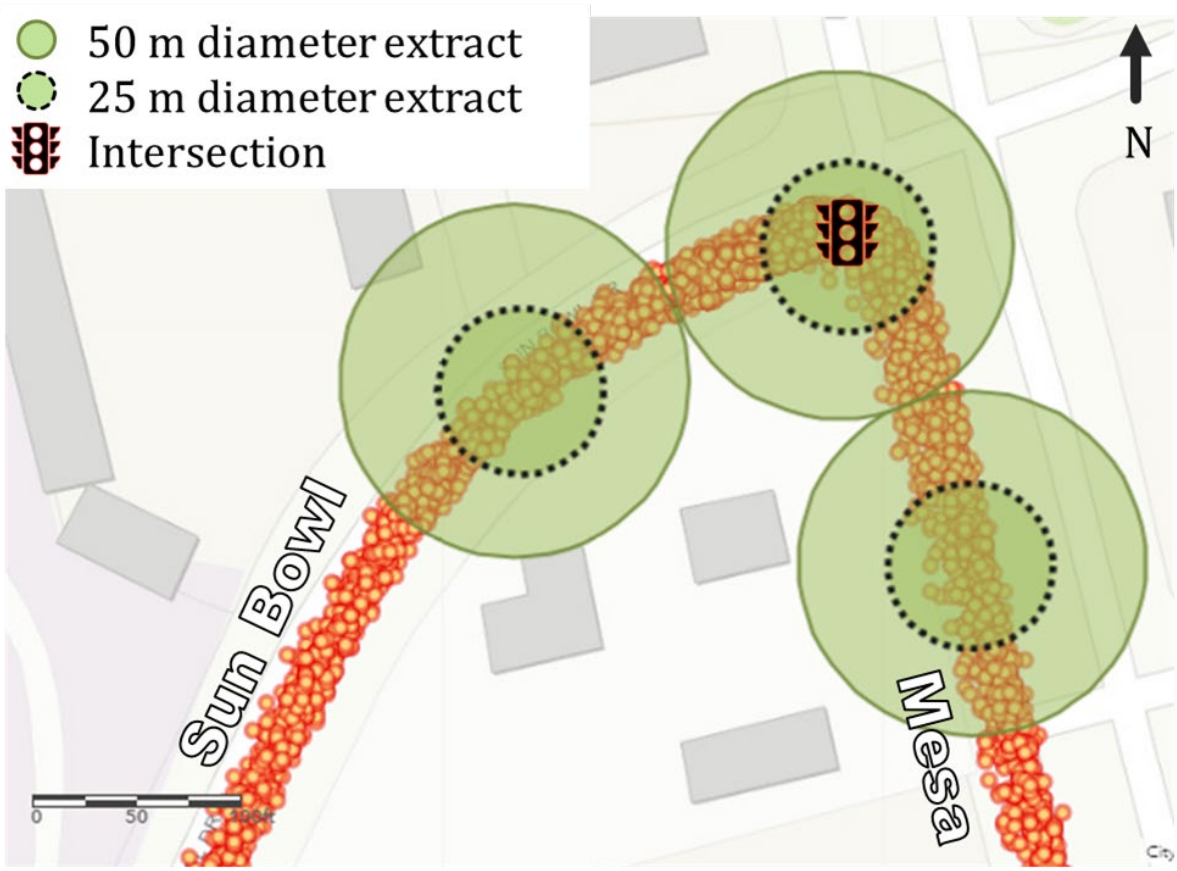

Figure 21 Intersection Analysis Example at Mesa and Sun Bowl

Figure 22 shows the time series for each pollutant data at the Mesa and Sun Bowl intersection throughout the course of the collection period. This data only reflects the mobile monitoring data, and as such is not a continuous set of data throughout the whole period and only has about 6 hours for each day.

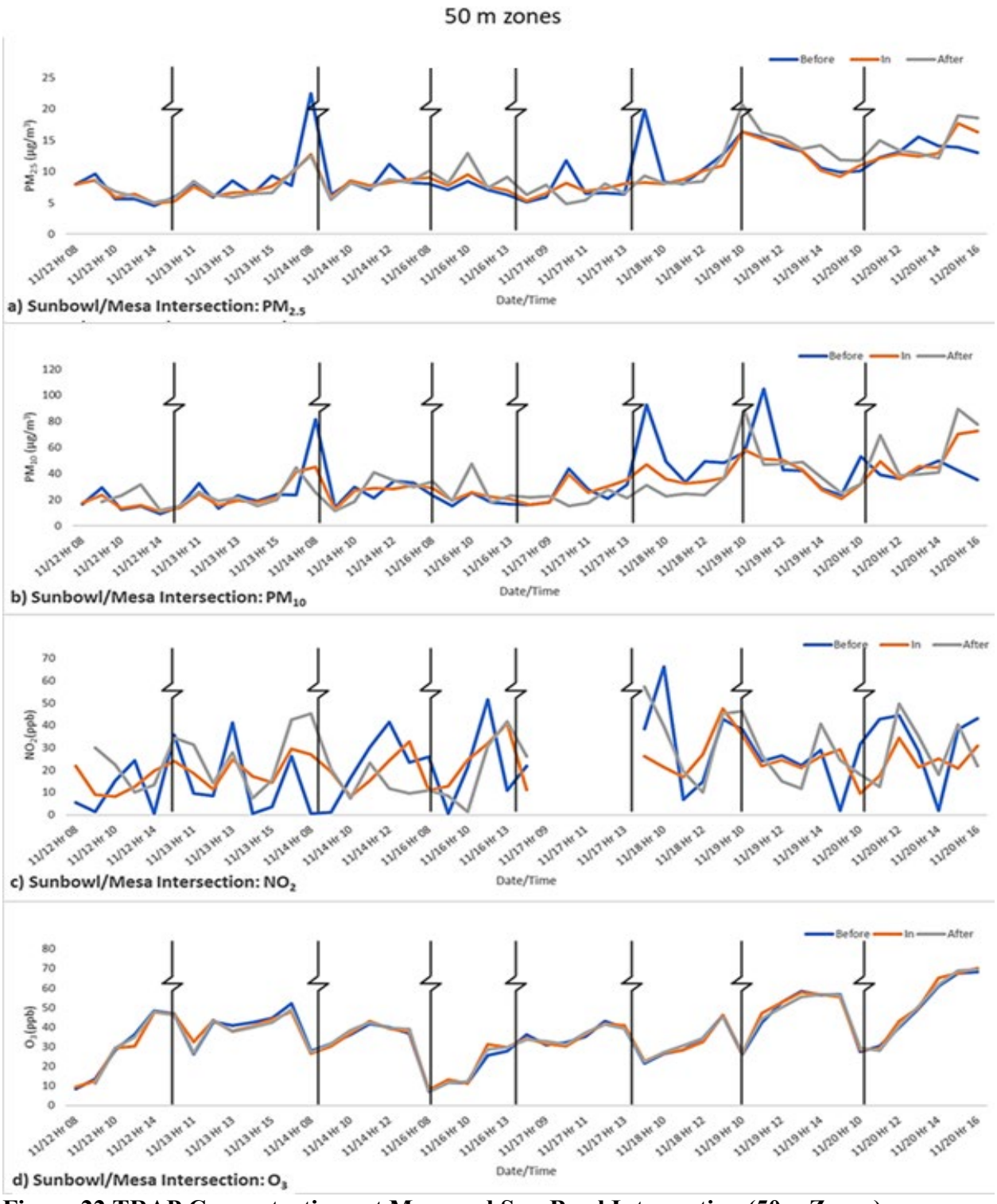

Figure 22 TRAP Concentrations at Mesa and Sun Bowl Intersection (50m Zones)

The greatest values of PM_{10} and $PM_{2.5}$ are observed in the location before the intersection. NO_2 values seem to fluctuate between being higher before and after the intersection but still showing greater values in the area before the intersection. O_3 values before, in, and after the intersection seem identical with no peaks observed at different parts of the intersection analysis.

Figure 23 shows the same analysis using 25-m diameter zones instead of 50 meters. The size of the zone was decreased to 25-m and no distinguishable difference was observed in the at-intersection and off-intersection concentrations for the four TRAPs. Figure 24 and Figure 25 show the 50 m zones intersection analyses at Schuster/Mesa and University/Mesa, respectively.

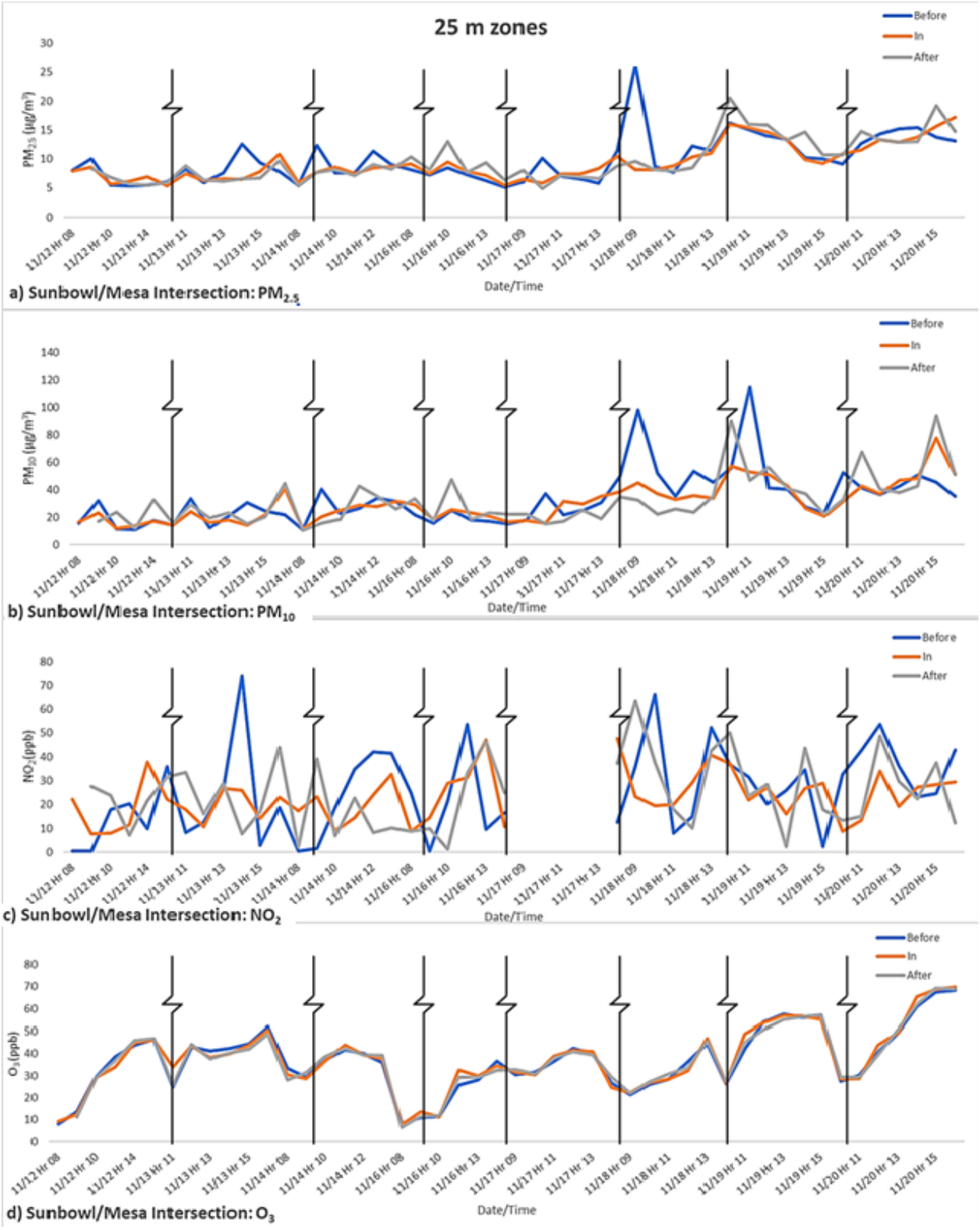

Figure 23 TRAP Concentrations at Mesa and Sun Bowl Intersection (25 m Zones)

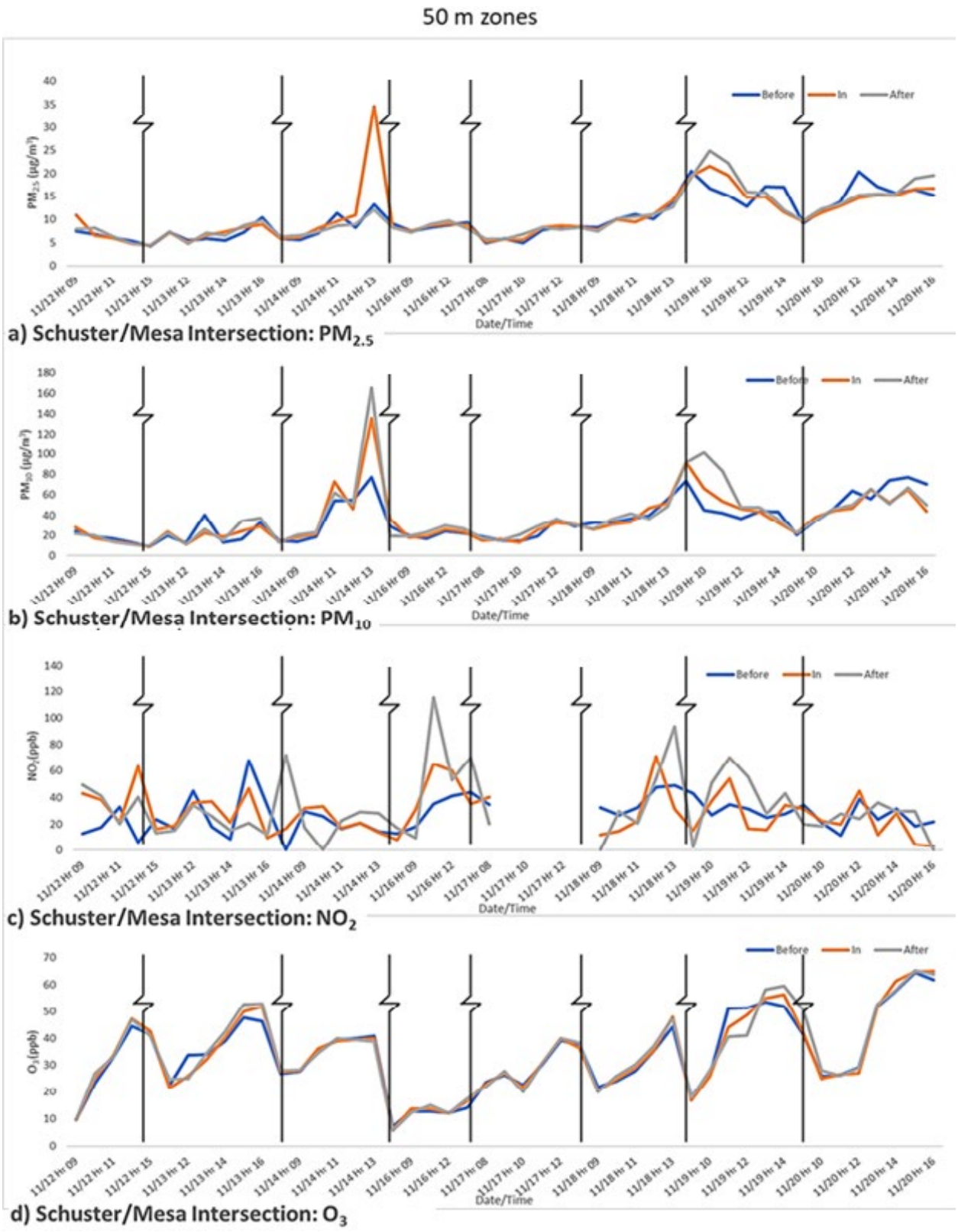

Figure 24 TRAP Concentrations at Mesa and Schuster Intersection (50 m Zones)

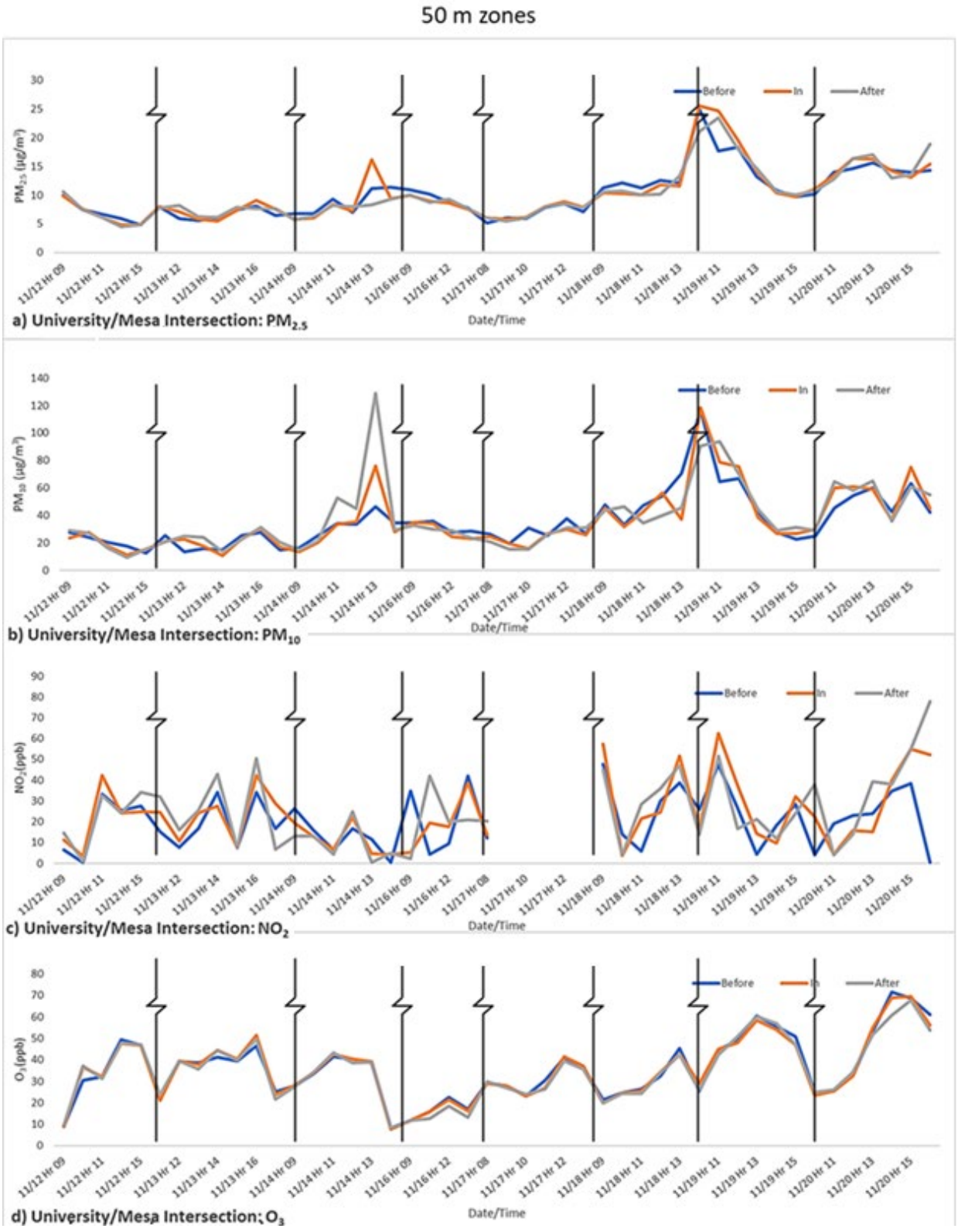

Figure 25 TRAP Concentrations at Mesa and University Intersection (50 m Zones)

Table 5 summarizes the intersection analysis with basic statistics. It can be seen that on average, pollutants concentrations are indistinguishable before, in, and after the intersection.

Table 5 Intersection Analysis Statistics (unit for PM: μg/m^3; NO_2 and O_3: ppb)

		Mesa/Sun Bowl 25 m			Mesa/Sun Bowl 50 m			Mesa/University 50 m			Mesa/Schuster 50 m		
		Avg	Max	Min	Avg	Max	Min	Avg	Max	Min	Avg	Max	Min
PM_{10}	Before	33.3	114.8	10.9	33.5	104.7	9.3	35.8	116.5	12.4	34.4	77.4	8.9
	In	30.2	77.6	11.8	31.4	72.6	11.2	35.8	118.5	10.9	35.5	135.6	9.0
	After	31.9	93.9	10.8	32.5	89.3	11.5	37.8	129.2	9.3	38.3	165.4	9.2
$PM_{2.5}$	Before	9.8	26.3	5.1	9.8	22.5	4.5	10.1	25.0	4.8	10.2	20.5	4.3
	In	9.2	17.2	5.3	9.3	17.7	5.0	10.3	25.5	4.8	10.7	34.6	4.4
	After	9.6	20.5	4.9	9.9	20.7	4.9	10.1	23.5	4.5	10.5	24.9	4.4
NO_2	Before	25.4	74.1	0.5	22.8	66.2	0.5	20.4	47.6	0.5	27.5	67.9	0.3
	In	23.0	47.6	7.7	22.1	47.5	8.3	23.7	62.5	3.5	29.0	71.1	3.3
	After	24.5	63.6	1.1	24.8	57.2	1.4	24.9	77.9	0.5	32.8	115.3	0.5
O_3	Before	36.9	68.2	8.2	37.0	68.2	8.0	35.6	71.7	8.4	33.8	64.4	7.1
	In	37.3	69.8	7.9	37.2	70.0	7.8	35.5	69.6	7.7	34.0	65.0	6.0
	After	37.5	69.2	6.5	37.6	69.5	6.8	34.8	67.7	8.2	34.4	65.2	5.7

4.2.4 Comparison of Stationary Site Measurements

Hourly pollutant values at the Sun Bowl site were compared to the CAMS 12 station located around 700 meters away shown in Figure 26. NO_2 values follow a similar pattern to the values collected at CAMS 12, while showing a few peaks higher than those reported at CAMS 12, occurring mostly in the evening. As is expected with the ubiquity of O_3, values between CAMS 12 and Sun Bowl are almost identical during the two-week period monitored.

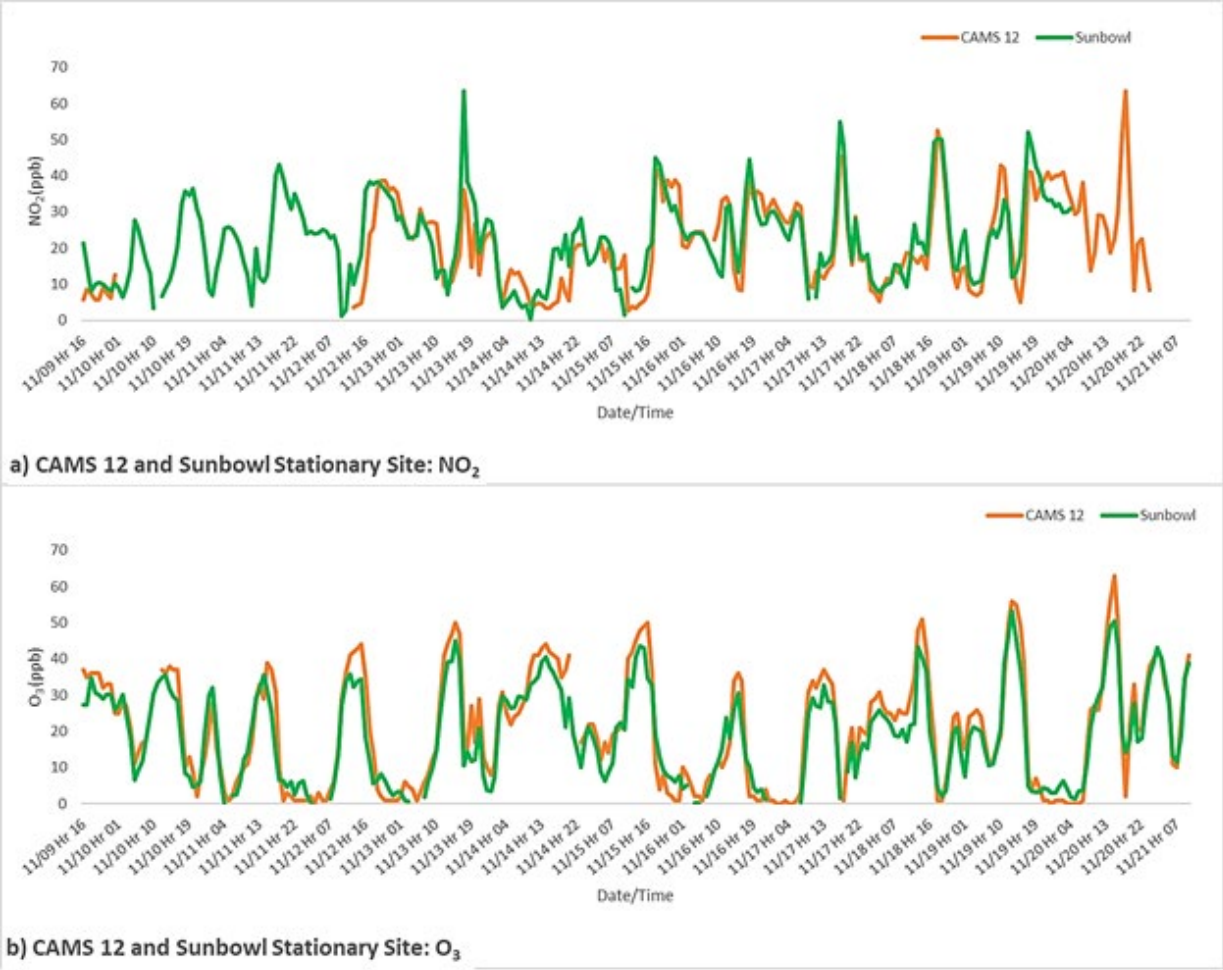

Figure 26 Comparison of NO_2 And O_3 Data Observed at Sun Bowl and CAMS 12

4.2.5 Comparison of Near-road and On-road Measurements

On-road measurements were compared to the near-road measurements observed at the two sites along the route. Since the on-road mobile monitor passed by the near-road sites for only a few seconds at a time, and near-road sites record data by the hour, all the instances of the on-road measurements by the near-road site during that hour were considered as the "on-road" measurement. It is observed that in general on-road shows strong relationship with fixed site data. The near-road site CAMS 12 is approximately 40 meters from the road and the Sun Bowl station was located much closer to the road segment at only 5 meters from the road. Figure 27 shows on-road measurements compared to near-road measurements at CAMS 12 and Sun Bowl. Data for PM at Sun Bowl were not included due to instrument malfunction.

Figure 27 On-road Monitoring and Near-Road Site

PM_{10} and $PM_{2.5}$ on-road measurements and those measured at the near-road site did not differ much at CAMS 12, with PM_{10} showing higher values than at near-road sites. On-road measurements of NO_2 were close to near-road measurements but had higher peaks at both sites and were generally higher than those measured at the Sun Bowl site. On-road measurements for O_3 were almost identical to near-road measurements at both sites. As established by other analyses in this study, O_3 is greatly ubiquitous in the area and only varies diurnally.

Figure 28 and Figure 29 show strong associations between the paired TRAP data (except NO_2) at CAMS 12 and Sun Bowl site, respectively.

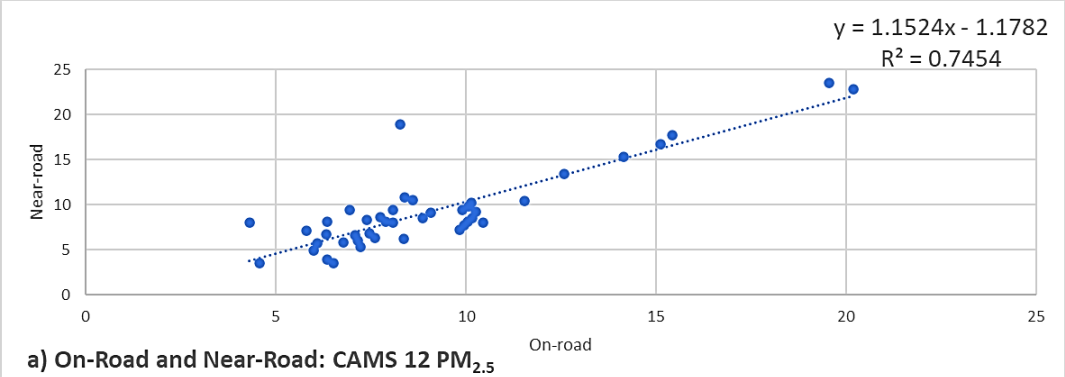

a) On-Road and Near-Road: CAMS 12 $PM_{2.5}$

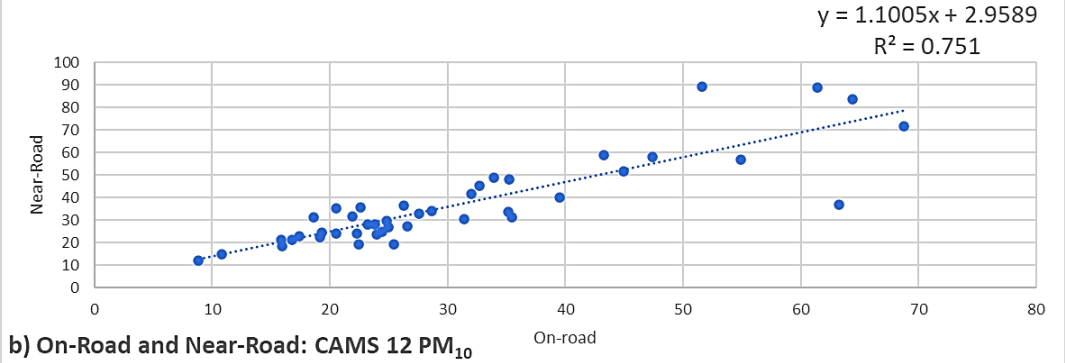

b) On-Road and Near-Road: CAMS 12 PM_{10}

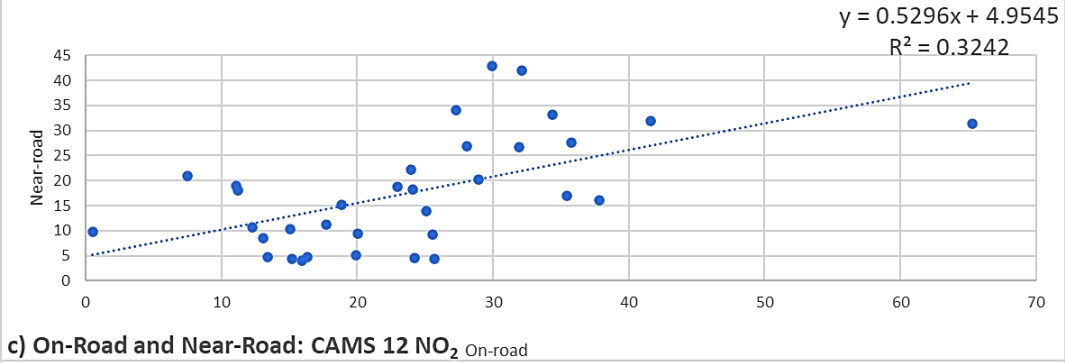

c) On-Road and Near-Road: CAMS 12 NO_2 On-road

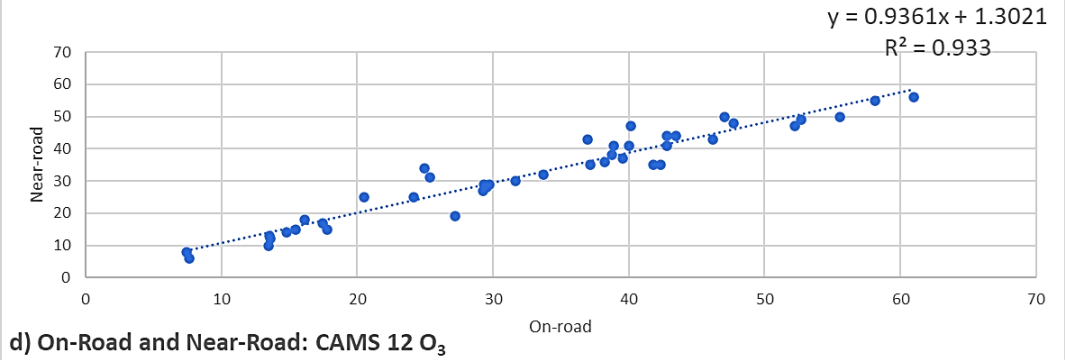

d) On-Road and Near-Road: CAMS 12 O_3

Figure 28 Pearson Correlations: CAMS 12

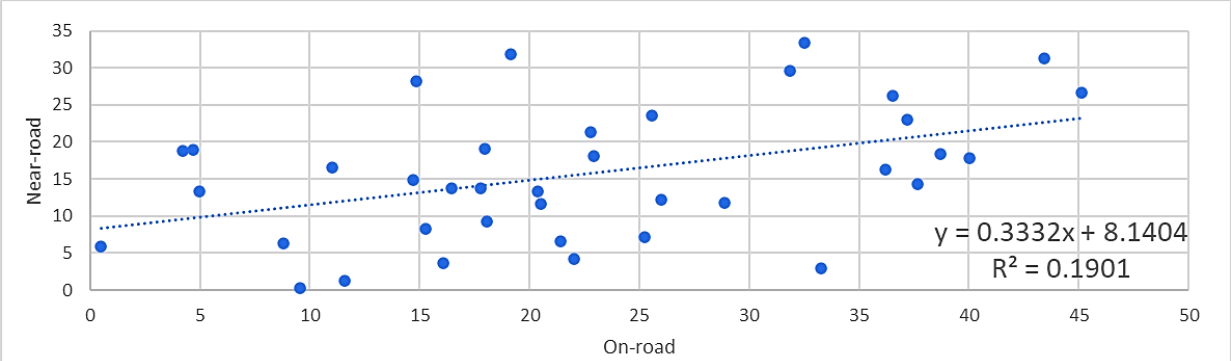

a) On-Road and Near-Road: Sun Bowl Stationary Site NO_2

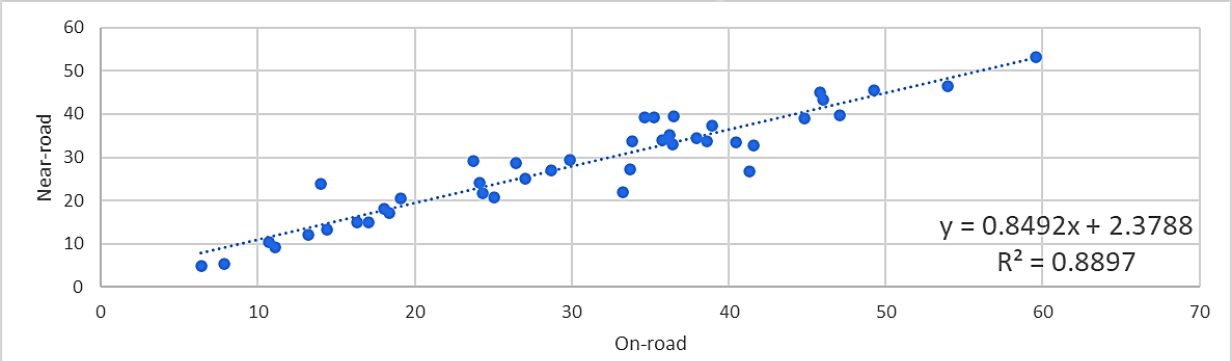

b) On-Road and Near-Road: Sun Bowl Stationary Site O_3

Figure 29 Pearson Correlations: Sun Bowl Stationary Site

4.3 Traffic Data and Emissions Modeling Results

The number of vehicles passing through the streets near Schuster Garage and Sun bowl parking location from November 7, 2021, to November 21, 2021, was compiled using a tube counting machine. Hourly averages were created for weekday days and weekend days and are shown in the following figure with all vehicle types classified. The tube counters and set-up of tubes allowed for monitoring of 14 different classes of vehicles. The hourly averages are shown in Figure 30. The vehicle count collected at one side of the Schuster count (C1- Schuster Garage) was missing, due to tube malfunctions throughout the study. However, one full day of data were collected properly and so the values from November 18, 2021, from 1:00 pm to November 19, 2021, to 12:00 pm were used to create ratios with vehicle counts from the opposing side of Schuster (C2- Schuster Garage). Using the profile of the 24 hours data, each hour divided by the count in the opposite direction to find the ratio. To approximate the correct values for C1-Schuster, the C1-Schuster values for the 24-hour data profile were divided by the values of the same period from C2-Schuster Parking. After the ratios were found, all the values from C2-Schuster were multiplied

to their respective time ratio to create a more concise value for the C1-Schuster data. The Sun Bowl Drive locations for traffic collection showed the correct data; therefore, no corrections were needed. Values for both ways of traffic flow at each site were added, and their average was taken for the hourly values and the time intervals.

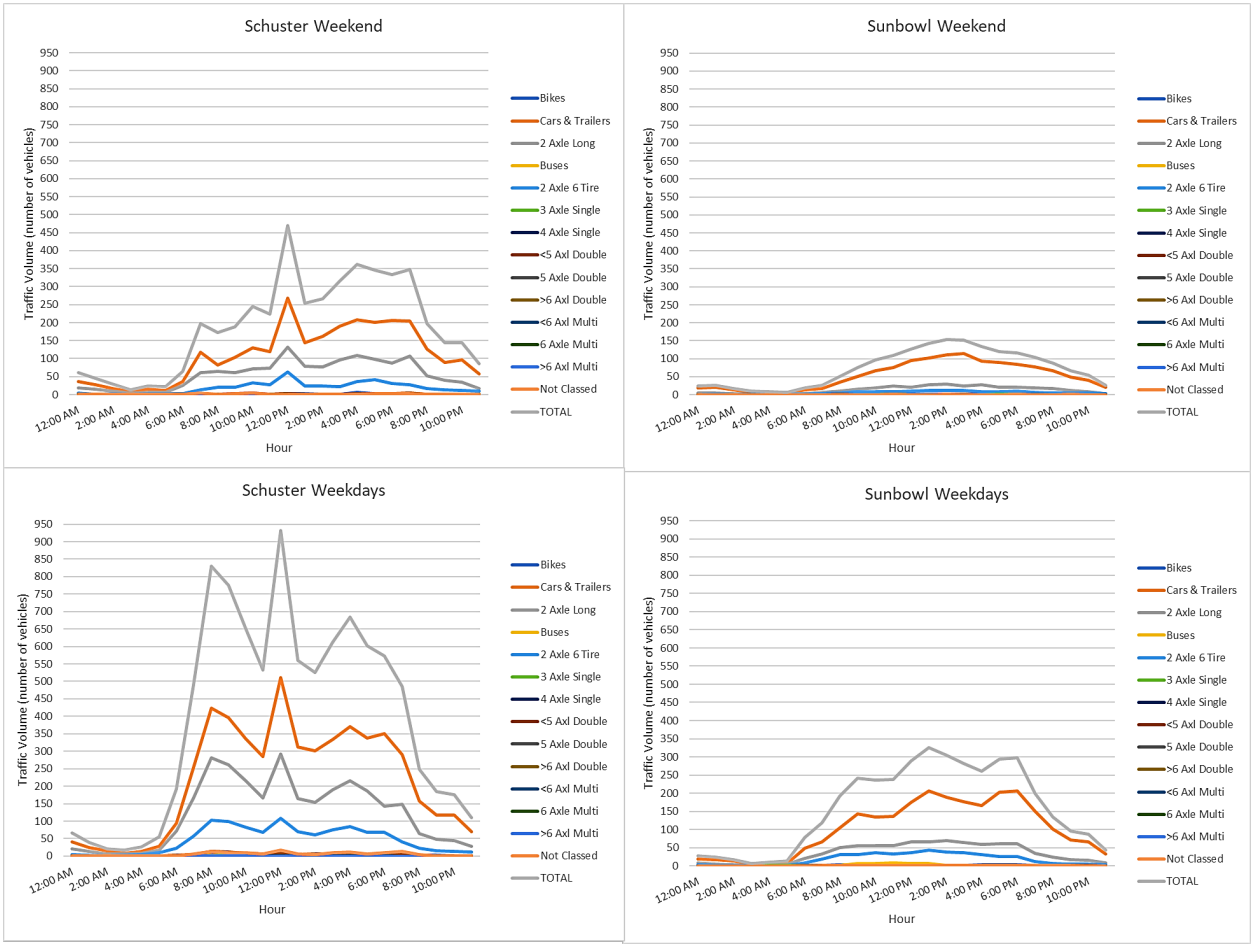

Figure 30 Hourly Traffic Counts for Weekday and Weekend

Weekday traffic appears to peak between 8am and 12pm and 6pm on both roads, with Sun Bowl Drive having only about half the traffic of Schuster Avenue. Weekend data on Schuster Avenue follows a similar pattern to the weekday data at about half the rate. Sun Bowl drive weekend data only peaks at around 2pm with no other major peaks and declines for the rest of the day.

Traffic volume data for all 14 vehicle classes combined is shown in Figure 31 for both Schuster Avenue and Sun Bowl Drive sites showing hourly averages for weekend and weekdays

during the study period. It can be seen that Schuster Avenue is about 3 times higher traffic volume than Sun Bowl Drive during both weekday and weekend time periods.

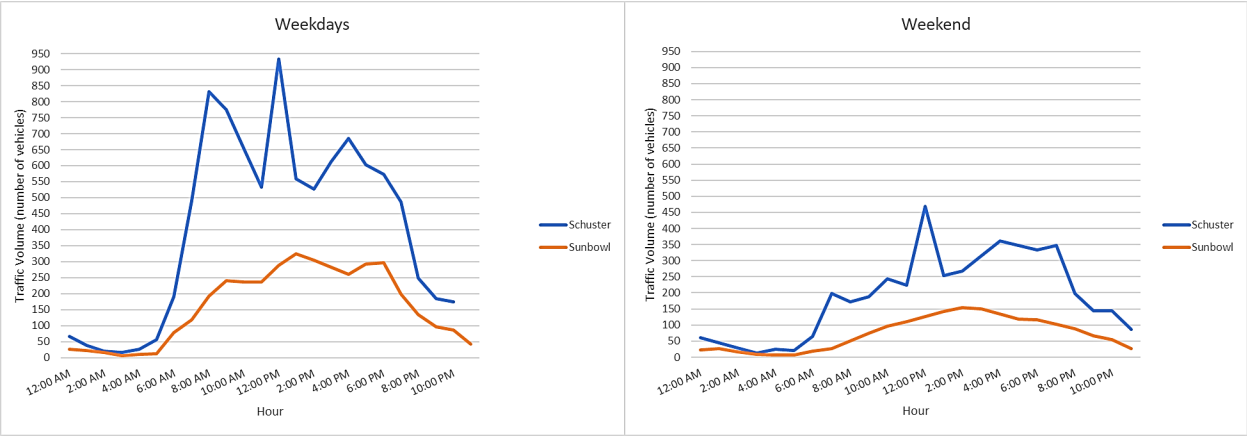

Figure 31 Combined Vehicle Classes Traffic Volume for Weekday and Weekend

4.3.1 MOVES3 modeling results

In order to process the traffic information in the emissions model MOVES3, the data were evaluated hourly and at different time intervals mentioned in Chapter 3. Hourly averages were created for each of the 4 time periods to be modeled in MOVES3. Vehicle classes from the tube counter data were converted into the 13 classes used by MOVES3. Once the vehicle classes were converted, vehicle fractions for each critical hour of the 4 time periods were found to provide the source type fractions required by MOVES3.

Emission inventories were calculated for the two links, Sun Bowl Drive (SB) and Schuster Avenue (SC), for the four time periods, for typical weekday and weekends in November. The emissions inventories are shown in Figure 32.

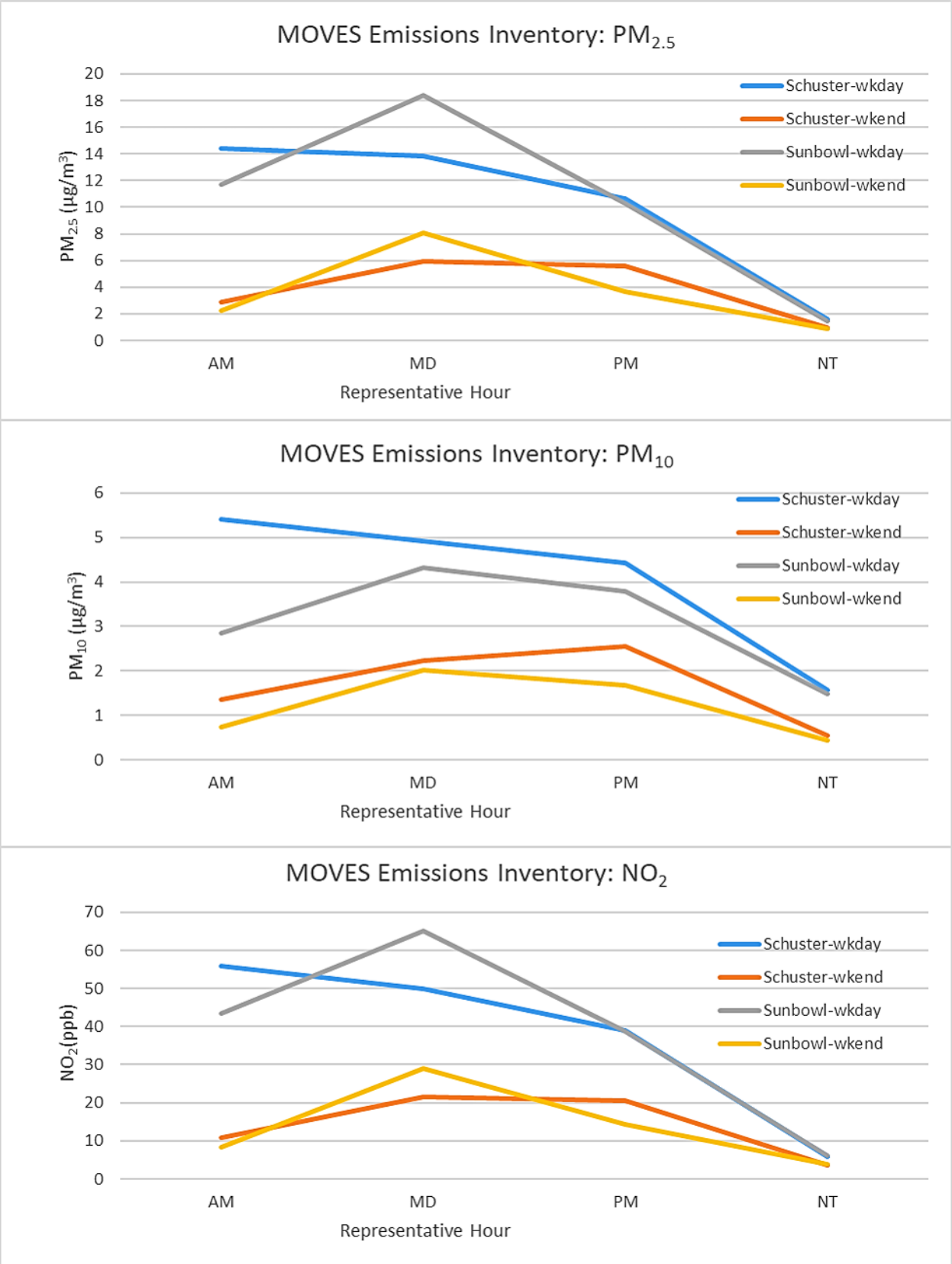

Figure 32 MOVES Emissions Inventories for Two Modeled Links

Modeling emissions inventories for these three pollutants provides an hourly estimate of emissions from these links without consideration for dispersion. As expected, these emissions are driven by the traffic volume at each peak hour. Estimated $PM_{2.5}$ emissions are twice as high as PM_{10} emissions, while observed measurements at stationary sites and on-road measurements indicate that PM_{10} is actually the higher value. This provides further evidence that PM_{10} is not driven by traffic-related emissions. NO_2 emissions predicted by MOVES3 indicate an increase in NO_2 at Morning (AM) and Midday (MD) hours, while observed values of NO_2 show peaks in the evening hours of the day. This is due to real-life conditions associated with the nitrogen dioxide photolytic cycle in which NO_2 and O_3 are interacting, and with the other nitrogen compounds that could also be present in these photochemical redox processes between the emission sources and road-side monitors.

CHAPTER 5 DISCUSSION

5.1 Spatial Averaging Near a Stationary Site

Each 1-second pollutant concentration data in this study represents the spatial average of an on-road pollutant concentration over a street length of approximately 9 to 14 m if the vehicle was moving, and less than 1 m if the vehicle was at a halt. Each trip took approximately 12 minutes and resulted in approximately 5 seconds of data (or 5 data points) of pollutant concentration in an hour for making a "pseudo collocated" comparison between the hourly averaged data measured at a stationary site and the on-road data recorded by the mobile monitor passing the site. To overcome the sparseness and to increase the representativeness of the on-road data for comparison with the data recorded at a stationary site, the mobile data were averaged over a longer route near a stationary site. For the comparison with the stationary site at Sun Bowl, an extended 130-m road was chosen to overcome the sparseness of the hourly mobile data passing by the Sun Bowl site. **Figure 33**a shows the road segment used in the analysis for the Sun Bowl site. As a result, a total number of up to 300 data points were used in developing an hourly mobile average at this location for each hour. Similarly, for the comparison with CAMS 12 data, the mobile data collected around a roughly 100-m by 100-m block (including 3 stop-and-go traffic intersections) was averaged to make a comparison with the recorded FRM data. **Figure 33**b shows the route used in developing a spatially averaged 1-hour pollutant concentration for comparison with the CAMS 12 data. As a result, a spatially averaged on-road data (around 300 data points) from the vicinity near CAMS 12 during the same hour was developed for making the comparison.

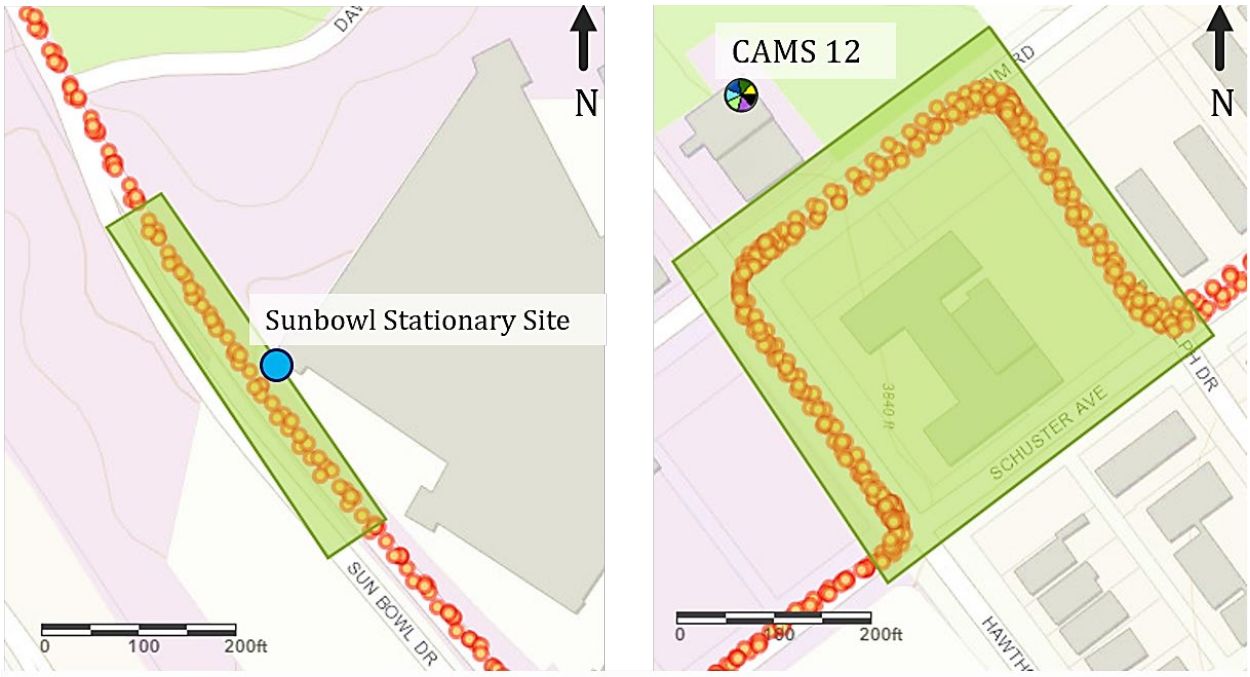

a) Spatially averaged points to compare on-road to near-road monitoring (Sunbowl)

b) Spatially averaged points to compare on-road to near-r monitoring (CAMS12)

Figure 33 Spatial Data Points Used for Estimating Hourly Average On-road Concentration Near a Stationary Site

The hourly mobile and stationary pollution data appear to agree very well with each other for all TRAPs in the two less travelled streets. Figure 27 shows that the magnitudes and the trends of the mobile PM data (both PM_{10} and $PM_{2.5}$) resemble closely with each other at CAMS 12. For a more ubiquitous TRAP such as O_3, the agreement is extremely well (Figure 27). The immediate, complicated photochemical reactions of NOx at tailpipe might have contributed to the incongruity between the on-road and near-road stationary data. Nevertheless, the hourly averaged NO_2 mobile data follows a similar trend and peaks concurrently as that observed at this site. On average, the on-road NO_2 concentration was higher than that monitored at a stationary station by 40%. Table 6 summarizes the correlation statistics for the on-road and near-road stationary data.

Table 6 Average, Percent Difference, and R^2: On-Road and Near-Road Sites

	Sun Bowl	On-road	Percent Diff.	R^2	CAMS 12	On-road	Percent Diff.	R^2
$PM_{2.5}$	NA	NA	-	-	10.4 µg/m³	9.9 µg/m³	-5%	0.75
PM_{10}	NA	NA	-	-	38.6 µg/m³	33.1 µg/m³	-14%	0.75
NO_2	15.4 ppb	22.8 ppb	48%	0.19	18.1 ppb	23.8 ppb	31%	0.32
O_3	29.5 ppb	32.1 ppb	9%	0.89	33.8 ppb	34.7 ppb	3%	0.93

The hourly mobile and stationary pollution data observed at the Sun Bowl site is shown in Figure 27. Again, the mobile and stationary O_3 data agree very well with each other and NO_2 data deviate from each other at this site. Stationary PM data for this site is not shown in the figure due to equipment malfunction at the beginning of the experiment. The O_3 data show excellent correlation between the two sets of data (Figure 27 and Table 6). NO_2 data observed by the mobile monitor again show higher values than those observed at a roadside stationary site. On-road NO_2 concentrations are strongly affected by local meteorology, photolysis of NO_2 and O_3, solar radiation, and tailpipe emissions from various types of vehicles. Traffic density and vehicle speed at Sun Bowl drive were quite different from that of CAMS 12 resulting, likely, higher deviations of the TRAPs between the on-road data and stationary road-side data.

5.2 Exposure Concentrations at Street Intersections

Street intersections in urban environment present a unique air quality scenario due to the street geometry induced turbulence, channeling effect on air flow, various vehicle exhaust conditions (engine, acceleration, braking, stop and go, idling, etc.), and different traffic (wait time and queue length) and road (surface roughness, waviness, serviceability) conditions at the intersections. A number of studies have been conducted to understand pollutant transport, dispersion, and removal near street intersections either by numerical simulation [34], [35] or field experiment. High PM mass and number concentrations have been reported near street intersections in urban environments [36], [37] but few studies have focused on the comparison of air quality data measured at street intersections and near-road stationary monitoring stations. In particular, comparison of on-road concentrations before entering and in a street-intersection has not been reported. Wang et al reported an average road-side NO_2 concentration of 18.6 ppb near a street intersection, compared to an average of 9.4 ppb reported from a nearby fixed station [38]. In another study, $PM_{2.5}$ concentrations at three setback locations 110-m, 330-m, and 500-m off an intersection were reported to be 7% lower than that measured at the street intersection, and 44% for CO [36]. This near flat $PM_{2.5}$ reduction gradient was attributed to high background PM concentrations and local meteorology, as was reported by deWinter et al [39] and Li et al [40].

Mobile TRAP concentrations were averaged over a zone of 50 m before, in, and after a street intersection, as shown in Figure 21. The time-series data are shown in Figure 22. The results show that the TRAP concentrations were indistinguishable immediately off and in the intersection.

A sensitivity analysis was conducted to evaluate if the size and location of the 50-m zone would have an impact on the spatio-temporal averaged concentrations and found no difference.

5.3 Limitations and Applications

Concurrent mobile and stationary monitoring of TRAPs using respective EPA FEM-designated instruments and a GPS tracking device equipped in the vehicle to provide real-time data of pollutant concentrations, coordinates of mobile measurements, and vehicle speed is demonstrated in this study. The corresponding spatial resolution for each measured pollutant concentration depends on the averaging time of the monitor and the vehicle speed. In this study, the minimum averaging times for PM, NO_2, and O_3 monitors are 6, 5, and 10 seconds, resulting in minimum spatial averages of approximately 60-m, 100-m, and 50-m for each of the recorded mobile concentration data, respectively. The 1-second average concentrations between two consecutive recorded readings were calculated by interpolation to yield concentration data representing a spatial average of approximately 10-m. The algorithm used in the interpolation would result in various degree of data smoothing and would also prevent the monitors from detecting the spatial variation within the minimum detection zone. A fast response device would help eliminate this deficiency, particularly if measurements are expected to take place on highways with higher speed limit.

The current study was conducted in a low traffic community during the 2020 SARS-CoV-2 pandemic in the U.S. where traffic conditions were significantly different from other places and other times. The vehicle speed was kept at 30 mph or lower under good traffic conditions. It is encouraging to observe that on-road monitoring provides data that are highly correlated to the data monitored at a stationary road-side monitor, whether the mobile data were aggregated from a neighboring block or a road segment near a stationary monitor. Mobile data may well represent the community exposure in a neighborhood where traffic emissions are less affected by the traffic and road conditions and where point sources are non-existing. In addition, the current study did not encounter any complicated emission condition such as cross-contamination from vehicle's own tailpipe emissions at traffic stops, traveling in the turbulent wake region behind a truck or clunker, halted in a traffic congestion, traveling in roadways impacted by other point sources, or traveling in adverse meteorological conditions. These circumstances would need to be addressed especially if a general guideline for on-road monitoring were to be developed. Furthermore, our study was

conducted during the day between 8 am and 5 pm. The data we have collected is not sufficient for making any conclusive comparison to 24-hr averaged or longer-term averaged concentrations, which are needed for most air quality or health effect studies.

Mobile real-time air monitoring provides a time lagged snapshot of air pollution over a large three-dimensional spatio-temporal concentration domain via a fast-moving vehicle. It has the advantages of covering a large domain in a short period of time and collecting data at locations that are difficult or impractical for system-wide stationary air monitoring such as near-road and on-road air monitoring. The advantages, however, are also coupled with disadvantages of not being able to record simultaneous observations at multiple locations and not being able to report sufficient data at a stationary location for exposure and health outcome assessments. Our study demonstrates that mobile air monitoring in a less travelled community can correctly detect the exposure concentrations that are representative of the community as well as near-road receptors.

CHAPTER 6: SUMMARY AND RECOMMENDATIONS

While efforts have been made to promote transit, walking, bicycling and other non-motorized transportation modes as a healthy lifestyle, the exposure of human to pollutants while carrying out these activities is yet to be fully understood. This project evaluated the feasibility of using transit vehicles traveling on fixed routes for near-road exposure assessment. Continuous on-road measurements of four TRAP pollutants (PM_{10}, $PM_{2.5}$, NO_2, and O_3) were recorded in conjunction with GPS locations. Concurrent near-road measurements at a project-established stationary site as well as a state-operated site monitoring data of the same pollutants were used to verify and provide associations with the mobile data. The data could be used to quantify exposures experienced by pedestrians, passengers, bus users, and near-road residents.

Part of this study focused on assessing the on-road data against that obtained at fixed stations. In general, on-road TRAP data recorded by the mobile monitors do not differ much from fixed site data. On-road measurements of NO_2 showed slightly higher values compared to near-road sites especially at a near-road site which is around 40 meters from the road and at an elevation difference of about 5 meters. On-road measurements compared to the data collected at the project-installed roadside monitor (5 meters away) showed much more similar values for NO_2.

It appears promising that community exposures to transportation pollutants can be represented by short-term spatio-temporal measurements using mobile air monitors. Spatio-temporal analysis showed the areas of concern for TRAPs without the need for multiple stationary sites. In general, near-road receptors are not affected by the traffic emissions and could be represented by on-road air monitors. Further research on how the mobile data can be used in exposure and health assessment and how the technique can be applied to characterize exposure concentrations at locations that stationary monitoring is not allowed or possible.

REFERENCES

[1] J. Aguilera *et al.*, "Land Use Regression of Long-Term Transportation Data on Metabolic Syndrome Risk Factors in Low-income Communities," 2021.

[2] L. V Giles and M. S. Koehle, "The health effects of exercising in air pollution.," *Sports Med.*, vol. 44, no. 2, pp. 223–249, Feb. 2014, doi: 10.1007/s40279-013-0108-z.

[3] K. W. Rundell and R. Caviston, "Ultrafine and fine particulate matter inhalation decreases exercise performance in healthy subjects.," *J. strength Cond. Res.*, vol. 22, no. 1, pp. 2–5, Jan. 2008, doi: 10.1519/JSC.0b013e31815ef98b.

[4] P. T. Cutrufello, J. M. Smoliga, and K. W. Rundell, "Small things make a big difference: particulate matter and exercise.," *Sports Med.*, vol. 42, no. 12, pp. 1041–1058, Dec. 2012, doi: 10.1007/BF03262311.

[5] N. A. H. Janssen, P. H. N. Van Vliet, H. Harssema, and B. Brunekreef, "Assessment of exposure to traffic relatedair pollution of.pdf," vol. 35, no. 2, pp. 3875–3884, 2001.

[6] A. Spira-Cohen, L. C. Chen, M. Kendall, R. Lall, and G. D. Thurston, "Personal exposures to traffic-related air pollution and acute respiratory health among Bronx schoolchildren with asthma.," *Environ. Health Perspect.*, vol. 119, no. 4, pp. 559–565, Apr. 2011, doi: 10.1289/ehp.1002653.

[7] S. Kingsley *et al.*, "Proximity of US Schools to Major Roadways: a Nationwide Assessment," *J. Expo. Sci. Environ. Epidemiol.*, vol. 24, Feb. 2014, doi: 10.1038/jes.2014.5.

[8] A. Iannuzzi *et al.*, "Air pollution and carotid arterial stiffness in children.," *Cardiol. Young*, vol. 20, no. 2, pp. 186–190, Apr. 2010, doi: 10.1017/S1047951109992010.

[9] R. X. Armijos, M. M. Weigel, O. B. Myers, W.-W. Li, M. Racines, and M. Berwick, "Residential exposure to urban traffic is associated with increased carotid intima-media thickness in children.," *J. Environ. Public Health*, vol. 2015, p. 713540, 2015, doi: 10.1155/2015/713540.

[10] F. D. Gilliland *et al.*, "The effects of ambient air pollution on school absenteeism due to respiratory illnesses.," *Epidemiology*, vol. 12, no. 1, pp. 43–54, Jan. 2001, doi: 10.1097/00001648-200101000-00009.

[11] L. Chen, B. L. Jennison, W. Yang, and S. T. Omaye, "Elementary school absenteeism and air pollution.," *Inhal. Toxicol.*, vol. 12, no. 11, pp. 997–1016, Nov. 2000, doi: 10.1080/08958370050164626.

[12] J. K. Wendt, E. Symanski, T. H. Stock, W. Chan, and X. L. Du, "Association of short-term increases in ambient air pollution and timing of initial asthma diagnosis among Medicaid-enrolled children in a metropolitan area," *Environ. Res.*, vol. 131, pp. 50–58, May 2014, doi: 10.1016/j.envres.2014.02.013.

[13] F. Barone-Adesi *et al.*, "Long-Term Exposure to Primary Traffic Pollutants and Lung Function in Children: Cross-Sectional Study and Meta-Analysis," *PLoS One*, vol. 10, no. 11, pp. e0142565–e0142565, Nov. 2015, doi: 10.1371/journal.pone.0142565.

[14] U. Gehring *et al.*, "Traffic-related air pollution and respiratory health during the first 2 yrs of life.," *Eur. Respir. J.*, vol. 19, no. 4, pp. 690–698, Apr. 2002, doi: 10.1183/09031936.02.01182001.

[15] D. Ierodiakonou *et al.*, "Ambient air pollution, lung function, and airway responsiveness in asthmatic children.," *J. Allergy Clin. Immunol.*, vol. 137, no. 2, pp. 390–399, Feb.

2016, doi: 10.1016/j.jaci.2015.05.028.
[16] J. Forns Guzman *et al.*, “Traffic-Related Air Pollution, Noise at School, and Behavioral Problems in Barcelona Schoolchildren: A Cross-Sectional Study,” *Environ. Health Perspect.*, vol. 124, Aug. 2015, doi: 10.1289/ehp.1409449.
[17] S. Lovinsky-Desir *et al.*, “Locations of Adolescent Physical Activity in an Urban Environment and Their Associations with Air Pollution and Lung Function.,” *Ann. Am. Thorac. Soc.*, vol. 18, no. 1, pp. 84–92, Jan. 2021, doi: 10.1513/AnnalsATS.201910-792OC.
[18] C. H. Yu, Z. Fan, P. J. Lioy, A. Baptista, M. Greenberg, and R. J. Laumbach, “A novel mobile monitoring approach to characterize spatial and temporal variation in traffic-related air pollutants in an urban community,” *Atmos. Environ.*, vol. 141, pp. 161–173, 2016, doi: https://doi.org/10.1016/j.atmosenv.2016.06.044.
[19] L. Minet, R. Gehr, and M. Hatzopoulou, “Capturing the sensitivity of land-use regression models to short-term mobile monitoring campaigns using air pollution micro-sensors.,” *Environ. Pollut.*, vol. 230, pp. 280–290, Nov. 2017, doi: 10.1016/j.envpol.2017.06.071.
[20] G. R. McKercher and J. K. Vanos, “Low-cost mobile air pollution monitoring in urban environments: a pilot study in Lubbock, Texas.,” *Environ. Technol.*, vol. 39, no. 12, pp. 1505–1514, Jun. 2018, doi: 10.1080/09593330.2017.1332106.
[21] P. Desouza, A. Anjomshoaa, F. Duarte, R. Kahn, P. Kumar, and C. Ratti, “Air Quality Monitoring Case Study Using Mobile Low-cost Sensors mounted on Trash-Trucks: Methods Development and Lessons Learned,” *Sustain. Cities Soc.*, vol. 60, p. 102239, 2020, doi: 10.1016/j.scs.2020.102239.
[22] Y. Wu, Y. Wang, L. Wang, G. Song, J. Gao, and L. Yu, “Application of a taxi-based mobile atmospheric monitoring system in Cangzhou, China,” *Transp. Res. Part D Transp. Environ.*, vol. 86, p. 102449, 2020, doi: https://doi.org/10.1016/j.trd.2020.102449.
[23] Y. Shi, K. K.-L. Lau, and E. Ng, “Developing Street-Level PM2.5 and PM10 Land Use Regression Models in High-Density Hong Kong with Urban Morphological Factors,” *Environ. Sci. Technol.*, vol. 50, no. 15, pp. 8178–8187, Aug. 2016, doi: 10.1021/acs.est.6b01807.
[24] A. A. Karner, D. S. Eisinger, and D. A. Niemeier, “Near-roadway air quality: Synthesizing the findings from real-world data,” *Environ. Sci. Technol.*, vol. 44, no. 14, pp. 5334–5344, 2010, doi: 10.1021/es100008x.
[25] A. Venkatram, M. Snyder, V. Isakov, and S. Kimbrough, “Impact of wind direction on near-road pollutant concentrations,” *Atmos. Environ.*, vol. 80, pp. 248–258, 2013, doi: 10.1016/j.atmosenv.2013.07.073.
[26] T. A. Cahill *et al.*, “Artificial ultra-fine aerosol tracers for highway transect studies,” *Atmos. Environ.*, vol. 136, pp. 31–42, 2016, doi: 10.1016/j.atmosenv.2016.03.058.
[27] 2B Technologies, “NO2/NO/NOx Monitor Operation Manual,” 2017.
[28] 2B Technologies, “Ozone Monitor Operation Manual,” 2017.
[29] GRIMM, “Specification for portable laser aerosol spectrometer and dust monitor Model 1.108/1.109,” *Users Man.*, p. 11, 2010.
[30] U.S. EPA, “Transportation Conformity Guidance for Quantitative Hot - spot Analyses in PM 2.5 and PM 10 Nonattainment and Maintenance Areas,” Office of Transportation and Air Quality, 2015.
[31] A. Horizon, M. T. Plan, and T. I. Program, “TRANSPORTATION CONFORMITY,” 2020.

[32] W. W. Li *et al.*, “Analysis of temporal and spatial dichotomous PM air samples in the El Paso-Cd. Juarez air quality basin,” *J. Air Waste Manag. Assoc.*, vol. 51, no. 11, pp. 1551–1560, 2001, doi: 10.1080/10473289.2001.10464377.
[33] J. H. García *et al.*, “Characterization and implication of potential fugitive dust sources in the Paso del Norte region,” *Sci. Total Environ.*, vol. 325, no. 1–3, pp. 95–112, 2004, doi: 10.1016/j.scitotenv.2003.11.011.
[34] L. Soulhac, V. Garbero, P. Salizzoni, P. Mejean, and R. J. Perkins, “Flow and dispersion in street intersections,” *Atmos. Environ.*, vol. 43, no. 18, pp. 2981–2996, 2009, doi: 10.1016/j.atmosenv.2009.02.061.
[35] M. F. Yassin, R. Kellnerová, and Z. Jaňour, “Impact of street intersections on air quality in an urban environment,” *Atmos. Environ.*, vol. 42, no. 20, pp. 4948–4963, 2008, doi: https://doi.org/10.1016/j.atmosenv.2008.02.019.
[36] Z. Wang, Q.-C. Lu, H.-D. He, D. Wang, Y. Gao, and Z.-R. Peng, “Investigation of the spatiotemporal variation and influencing factors on fine particulate matter and carbon monoxide concentrations near a road intersection,” *Front. Earth Sci.*, vol. 11, no. 1, pp. 63–75, 2017, doi: 10.1007/s11707-016-0564-5.
[37] N. Yu, S. Shu, Y. Lin, and Y. Zhu, “Assessing and reducing fine and ultrafine particles inside Los Angeles taxis,” *Atmos. Environ. J.*, vol. 181, no. February, pp. 155–163, 2018, doi: 10.1016/j.atmosenv.2018.03.023.
[38] A. Wang, M. Fallah-Shorshani, J. Xu, and M. Hatzopoulou, “Characterizing near-road air pollution using local-scale emission and dispersion models and validation against in-situ measurements,” *Atmos. Environ.*, vol. 142, no. 2, pp. 452–464, 2016, doi: 10.1016/j.atmosenv.2016.08.020.
[39] J. DeWinter, S. Brown, A. Seagram, K. Landsberg, and D. Eisinger, “A national-scale review of air pollutant concentrations measured in the U.S. near-road monitoring network during 2014 and 2015,” *Atmos. Environ.*, vol. 183, Apr. 2018, doi: 10.1016/j.atmosenv.2018.04.003.
[40] W.-W. Li, M. C. Chavez, I. Ramirez, and K. R. Cheu, “Assessing children’s spatiotemporal exposure to transportation pollutants in near-road communities,” Washington, D.C., 2019.

APPENDIX A – CALIBRATION

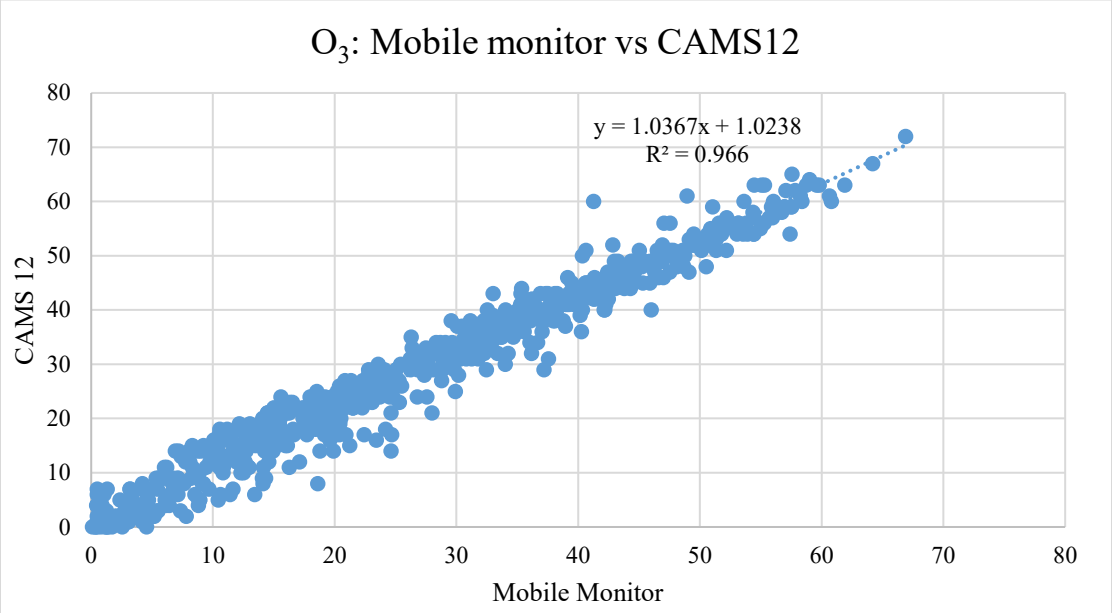

Figure A- 1 O_3 Correlation Plot: Mobile Monitor VS CAMS 12 FRM Data During Calibration Periods Before and After Study

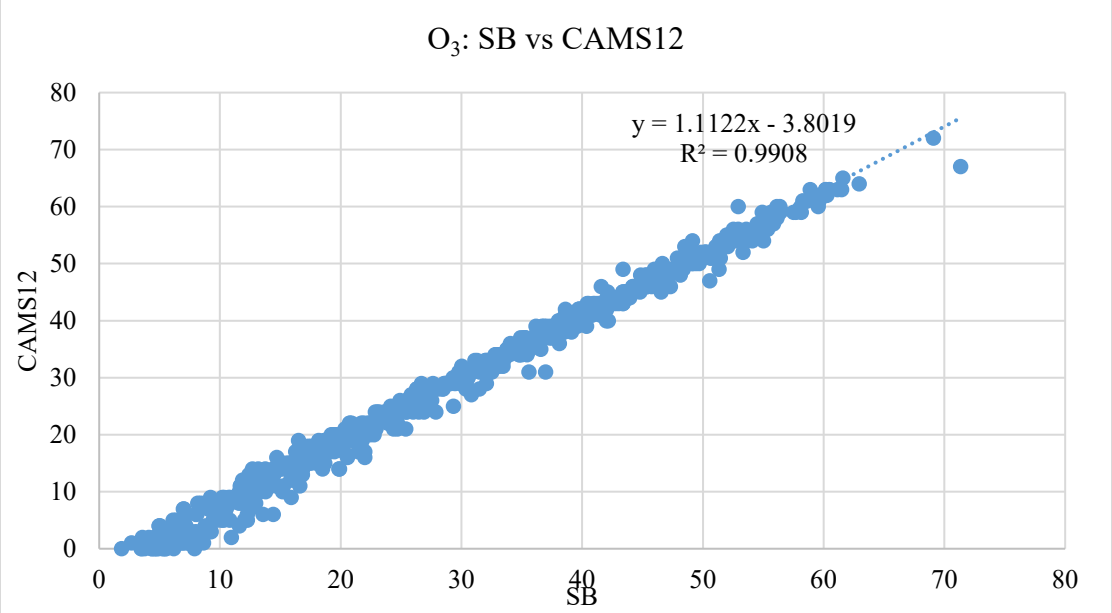

Figure A- 2 O_3 Correlation Plot: Sun Bowl (SB) Monitor Vs CAMS 12 FRM Data During Calibration Periods Before and After Study

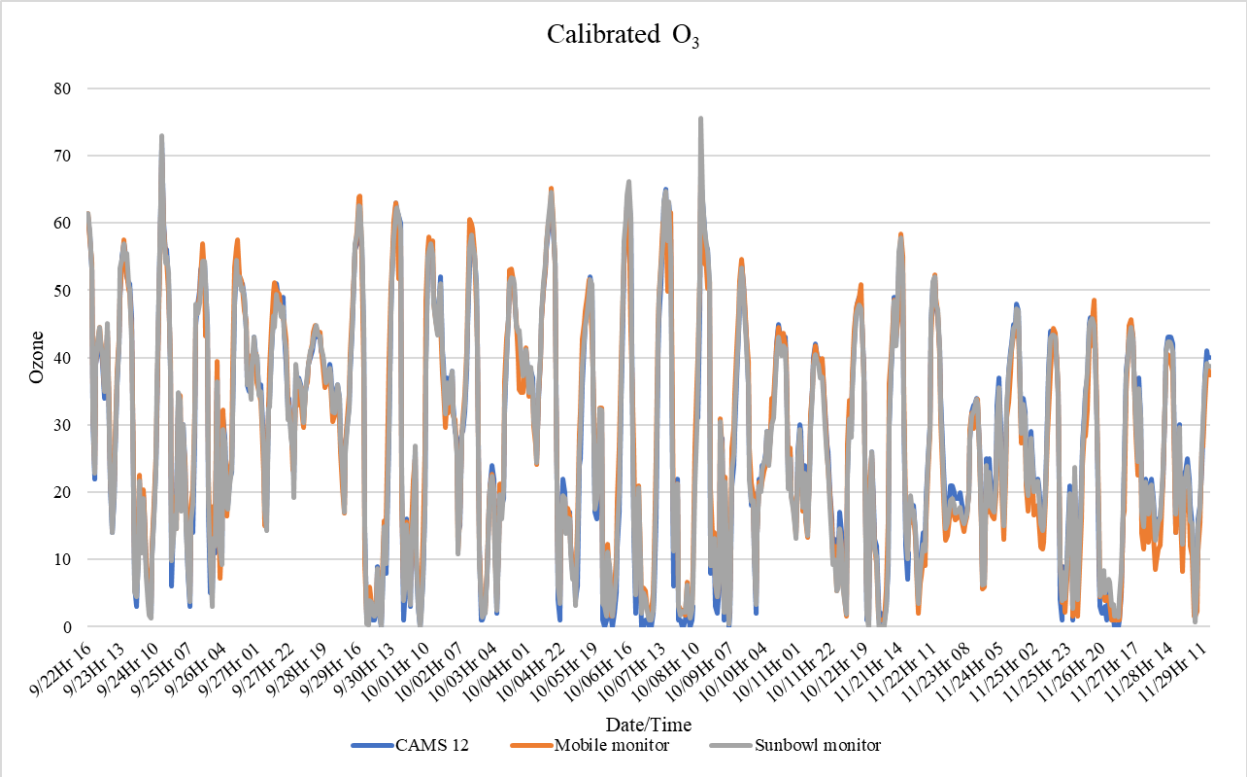

Figure A- 3 Calibrated O_3 Time Series

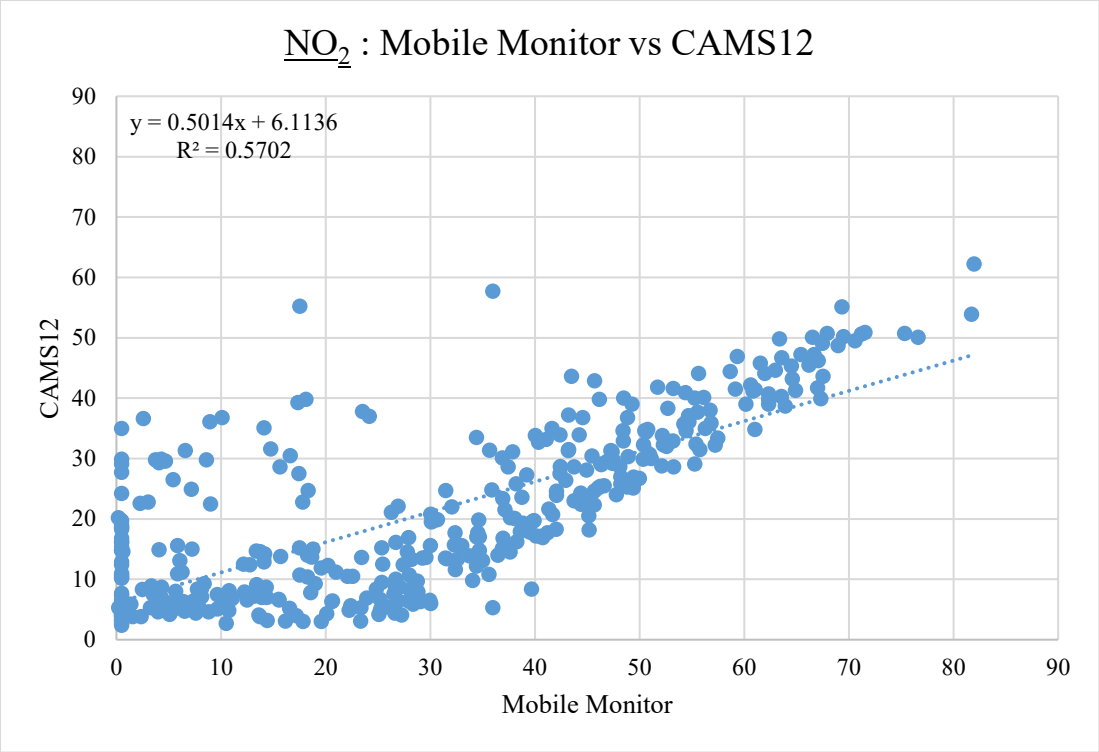

Figure A- 4 NO_2 Correlation Plot: Mobile Monitor VS CAMS 12 FRM Data During Calibration Periods Before and After Study

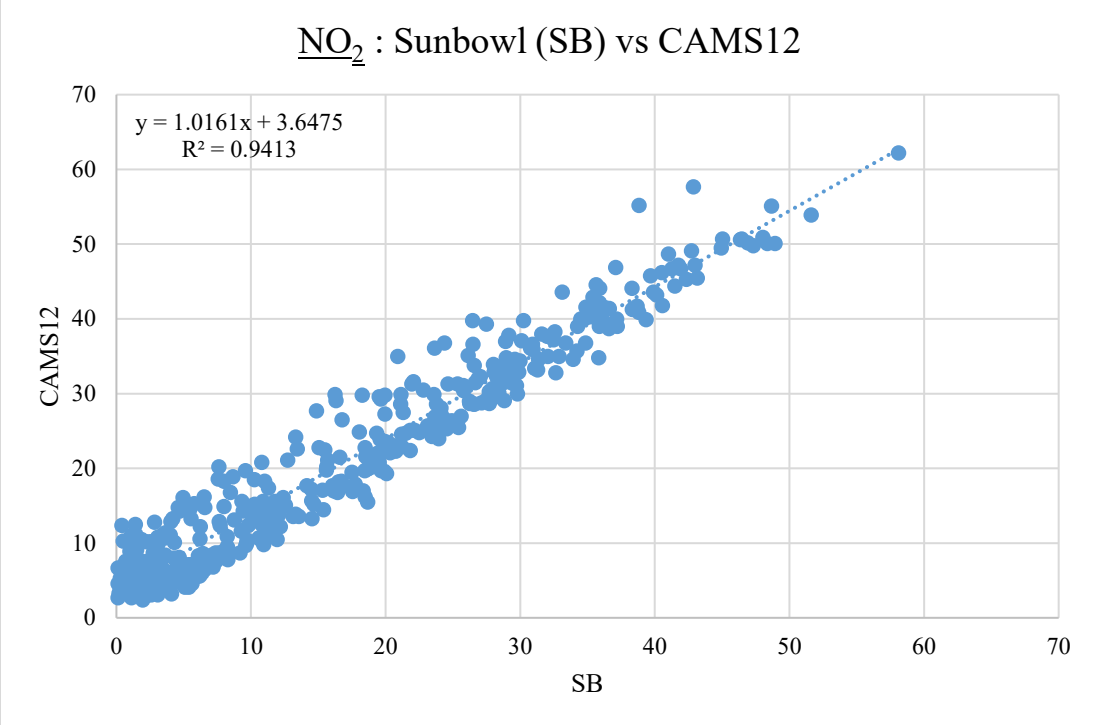

Figure A- 5 NO_2 Correlation Plot: Sun Bowl (SB) Monitor VS CAMS 12 FRM Data During Calibration Periods Before and After Study

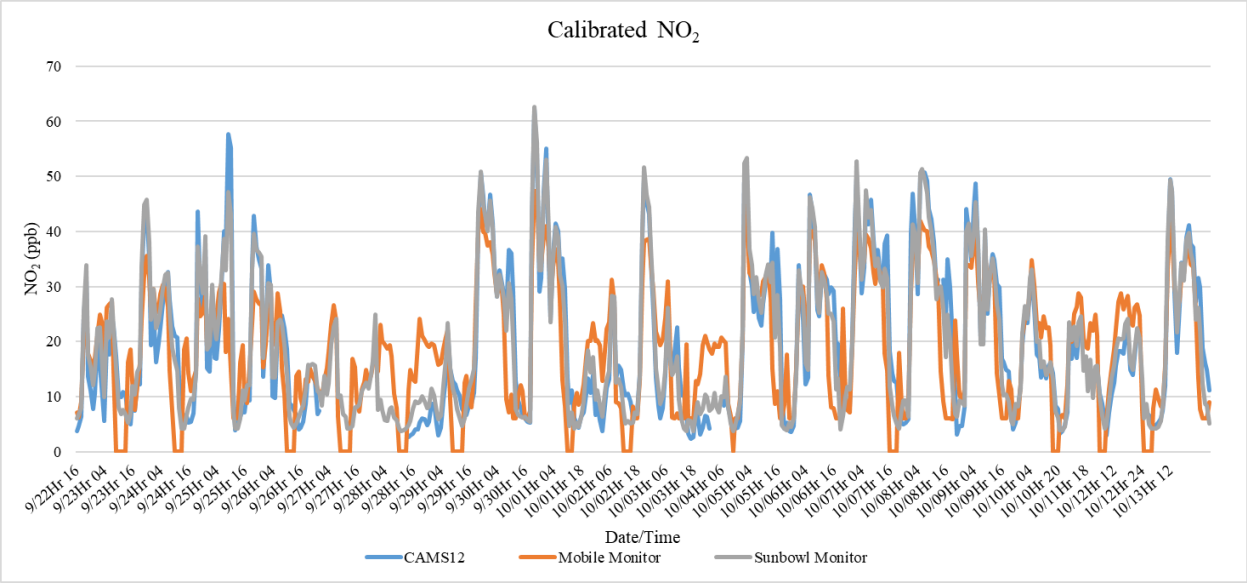

Figure A- 6 Post-Calibration NO_2 Time Series

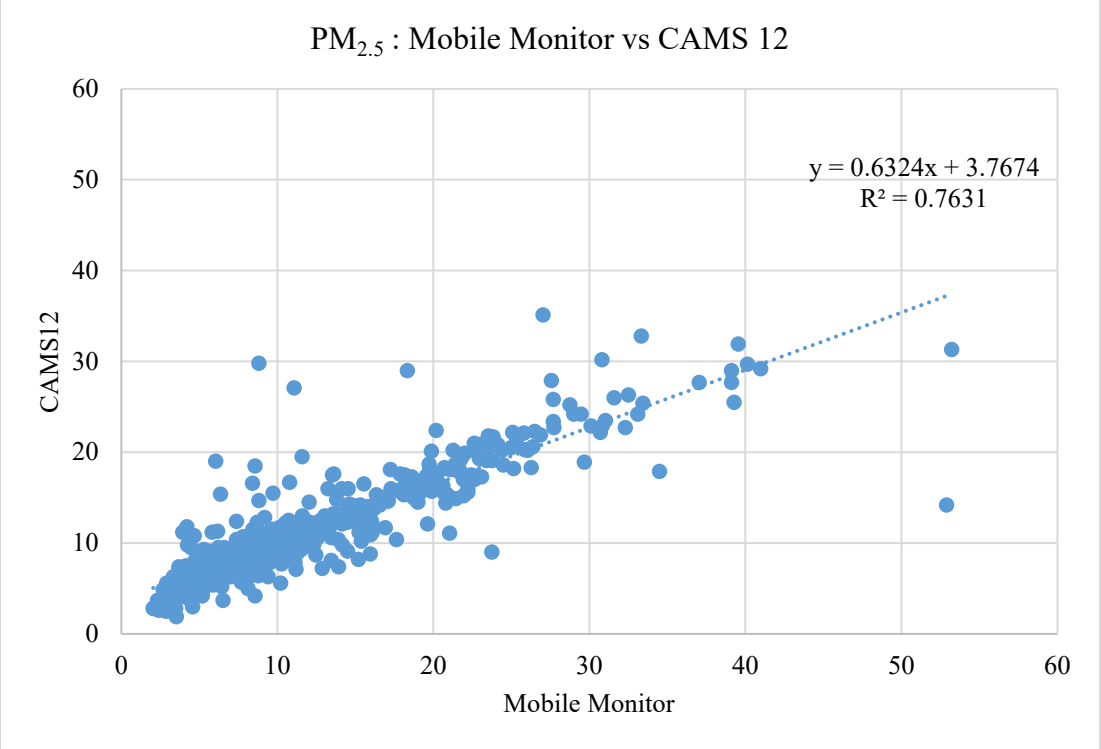

Figure A- 7 $PM_{2.5}$ Correlation Plot: Mobile Monitor Vs CAMS 12 FRM Data During Calibration Periods Before and After Study

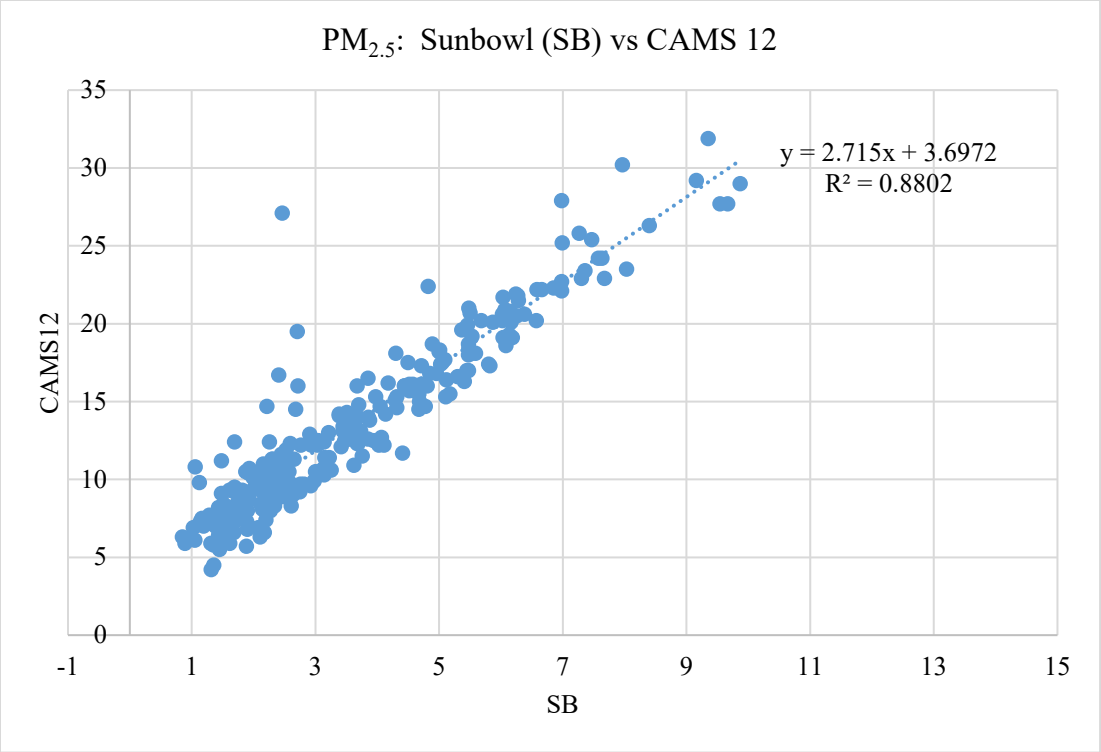

Figure A- 8 $PM_{2.5}$ Correlation Plot: Sun Bowl (SB) Vs CAMS 12 FRM Data During Calibration Periods Before and After Study

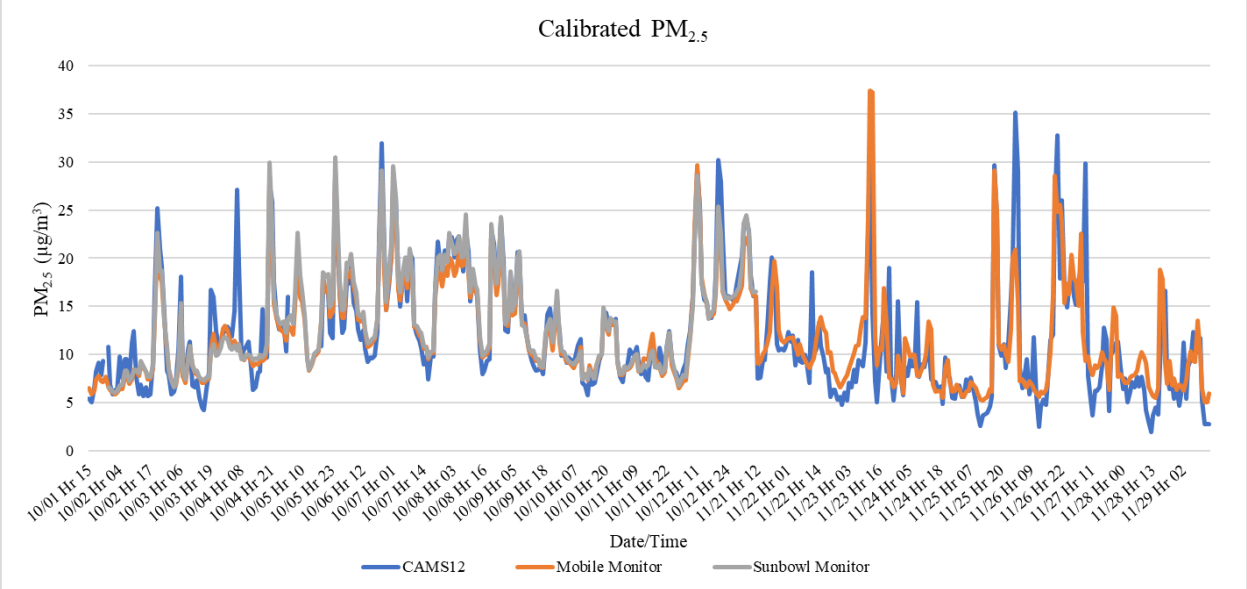

Figure A- 9 Calibrated $PM_{2.5}$ Time Series

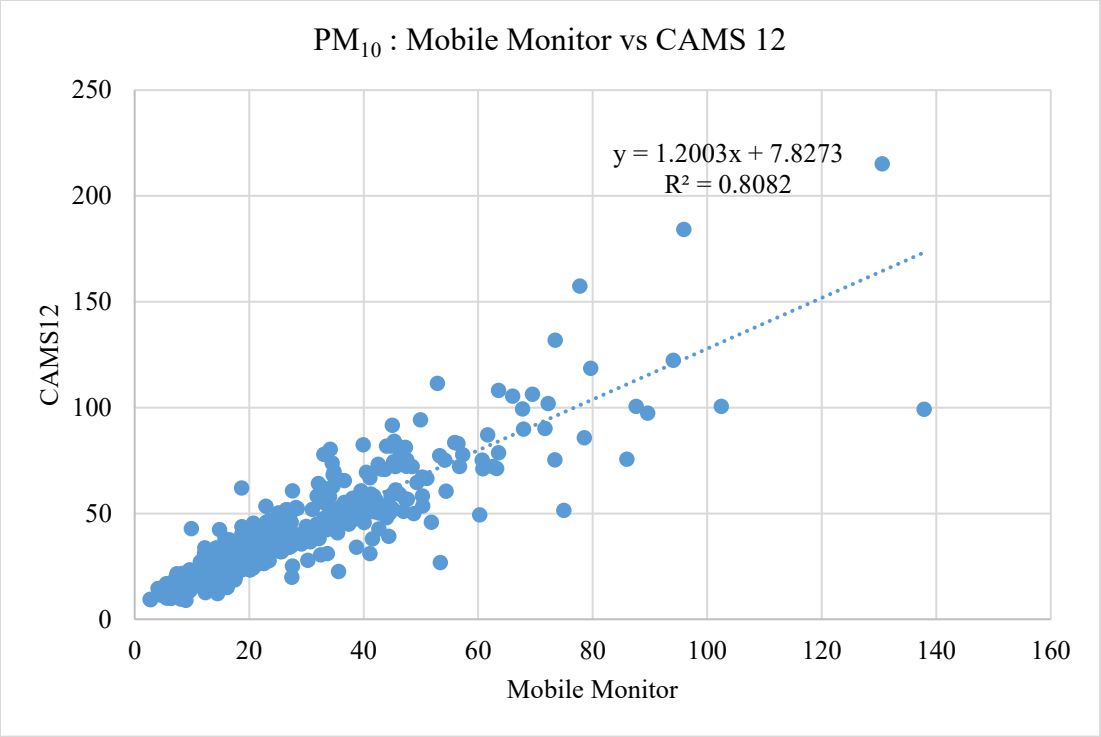

Figure A- 10 PM_{10} Correlation Plot: Mobile Monitor Vs CAMS 12 FRM Data During Calibration Periods Before and After Study

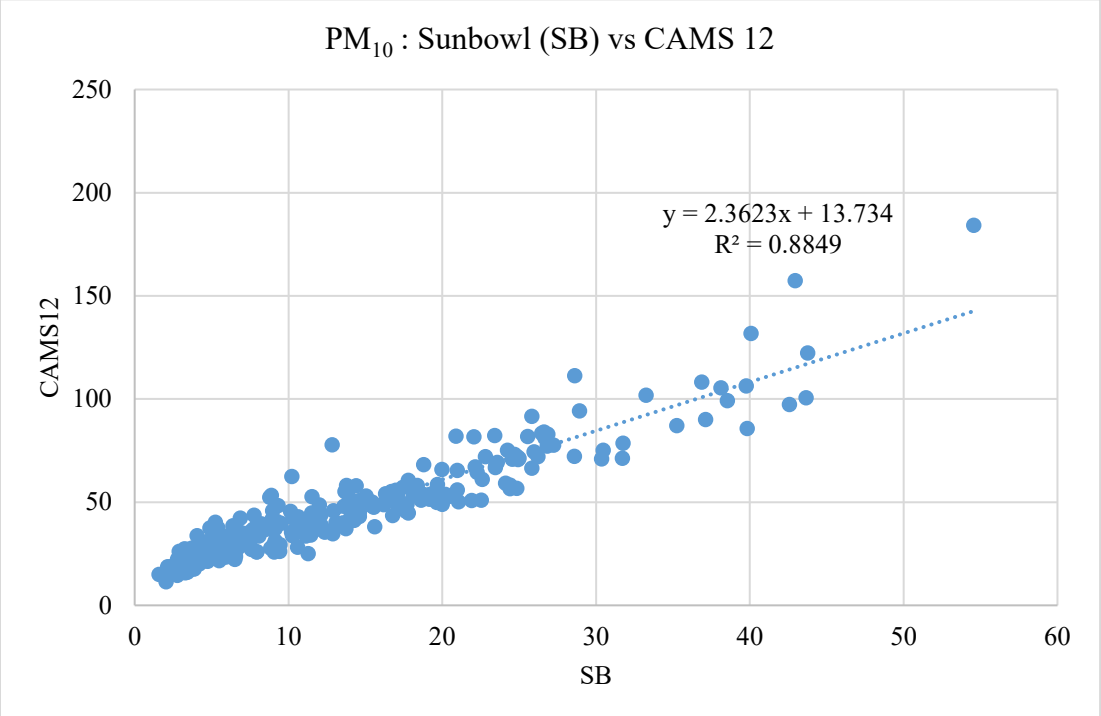

Figure A- 11 PM_{10} Correlation Plot: Sun Bowl (SB) Vs CAMS 12 FRM Data During Calibration Periods Before and After Study

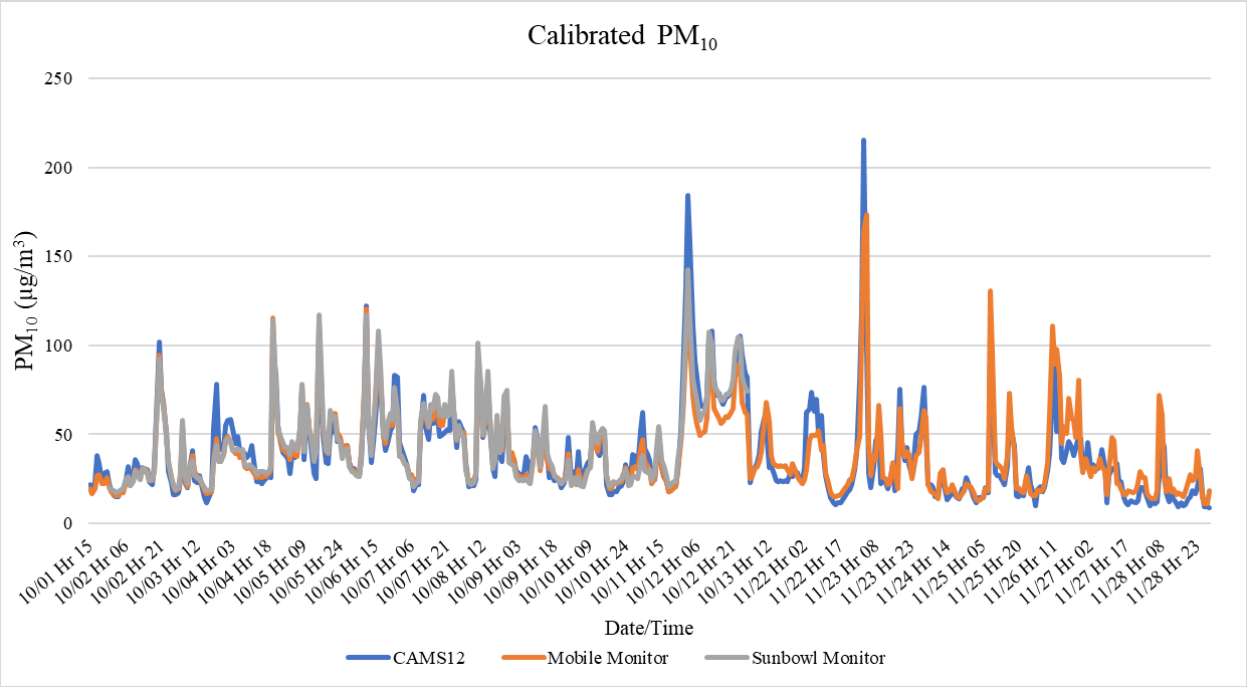

Figure A- 12 Calibrated PM_{10} Time Series

APPENDIX B- HOURLY BOXPLOT

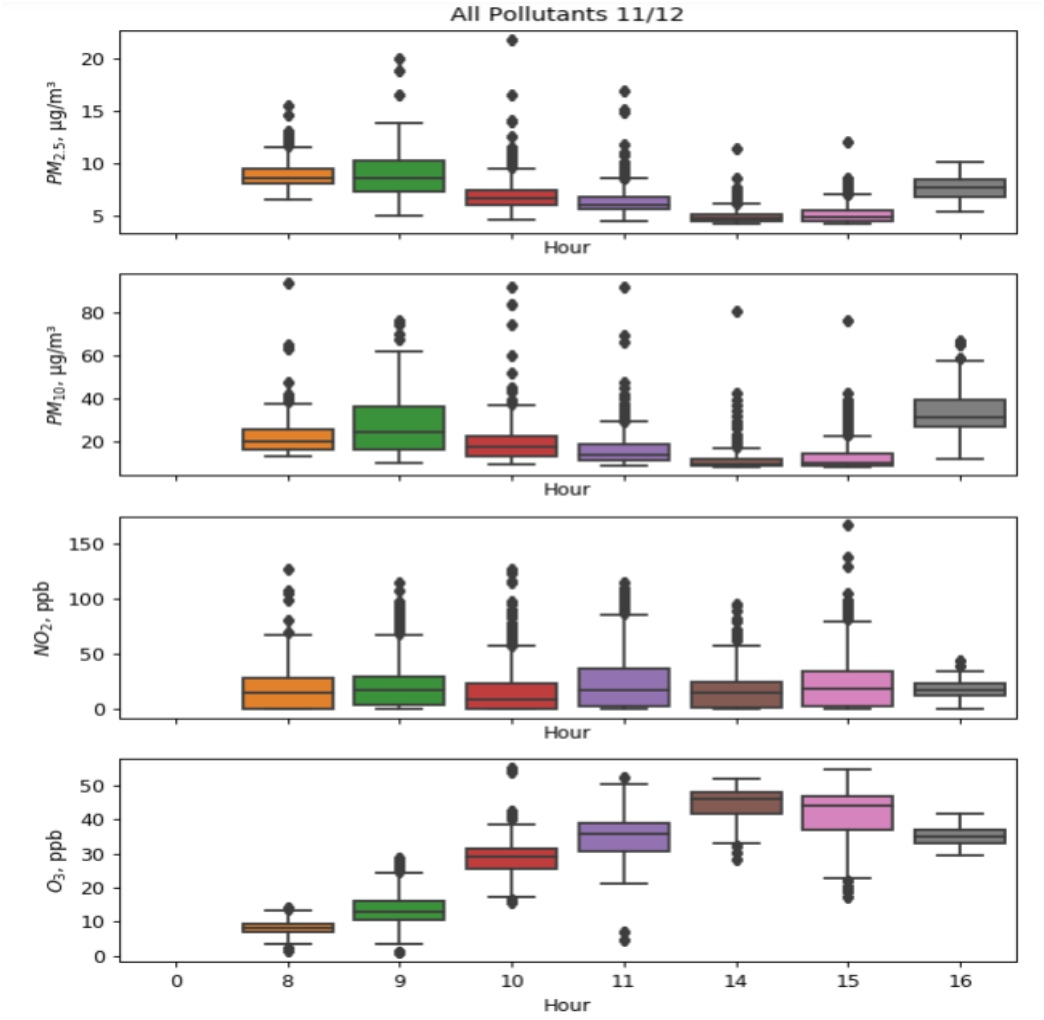

Figure B- 1 Hourly Boxplot: Pollutant Data For 11/12

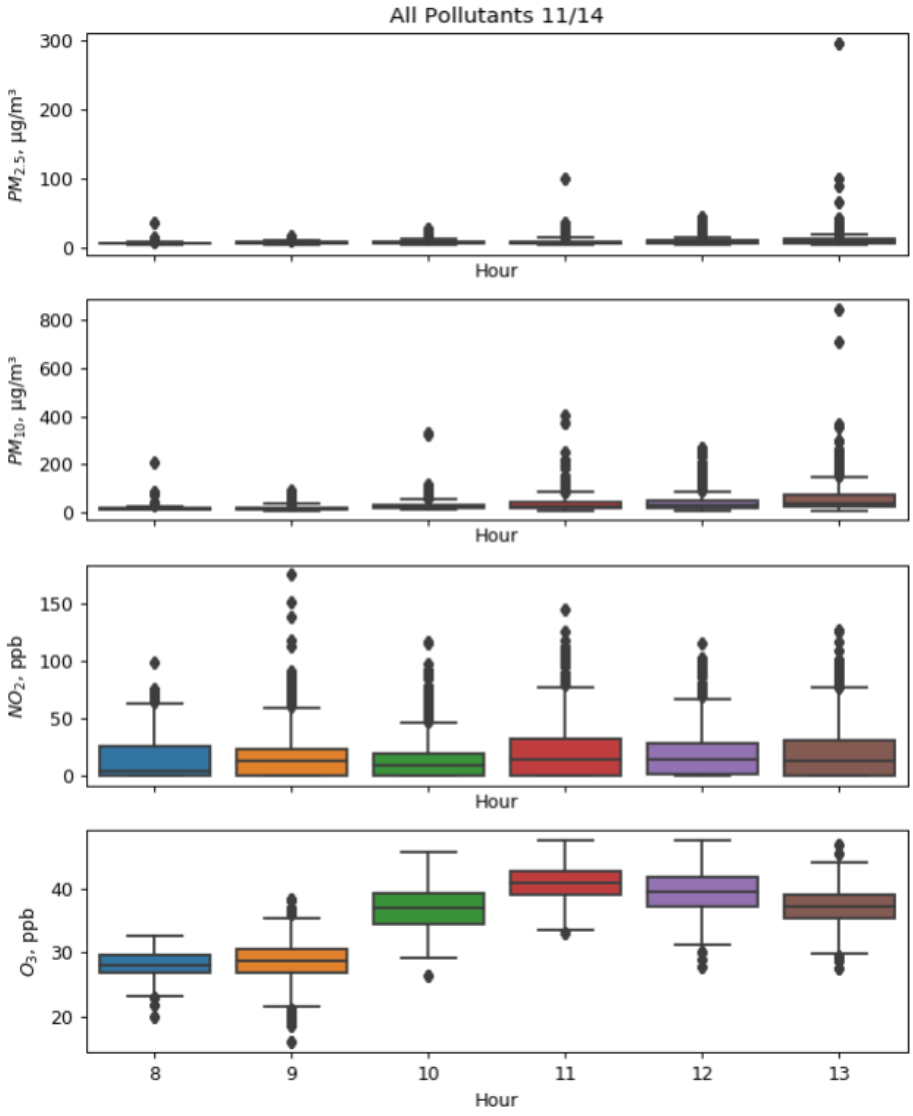

Figure B- 2 Hourly Boxplot: Pollutant Data For 11/14

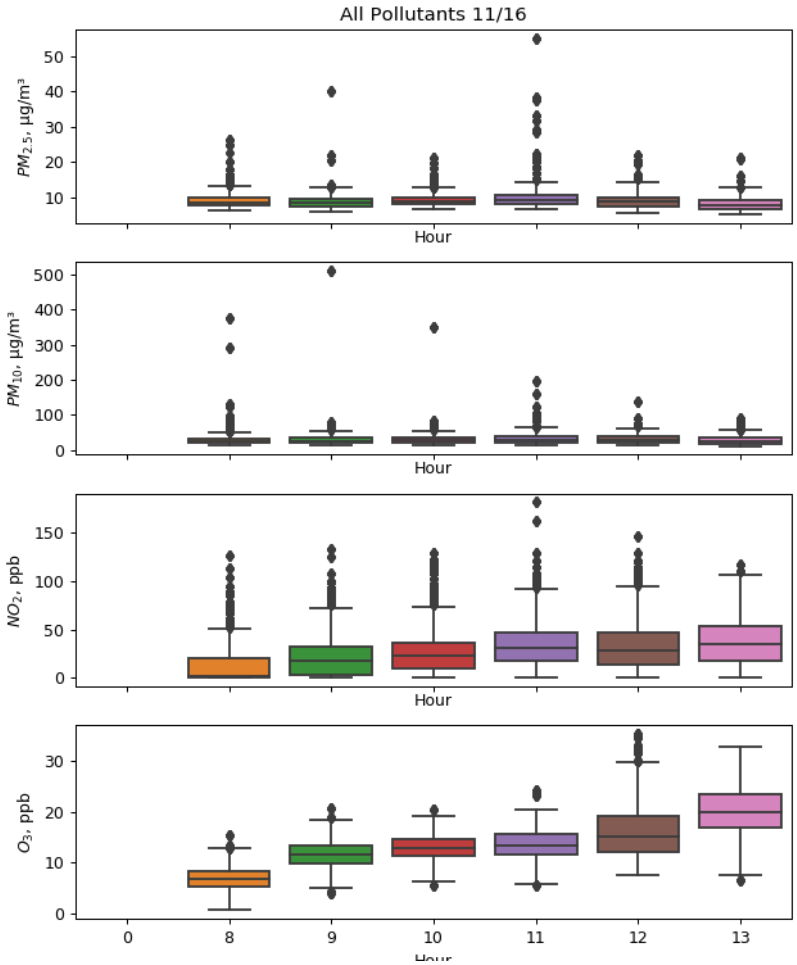

Figure B- 3 Hourly Boxplot: Pollutant Data For 11/16

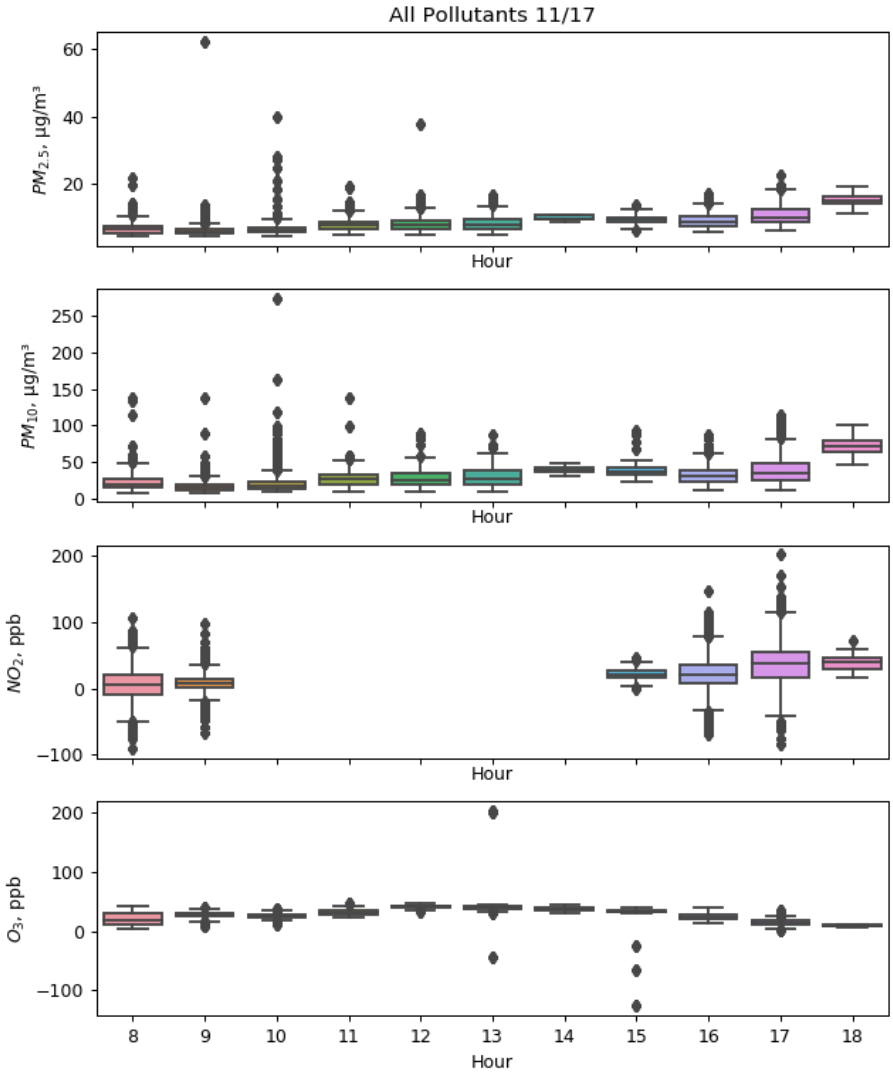

Figure B- 4 Hourly Boxplot: Pollutant Data For 11/17

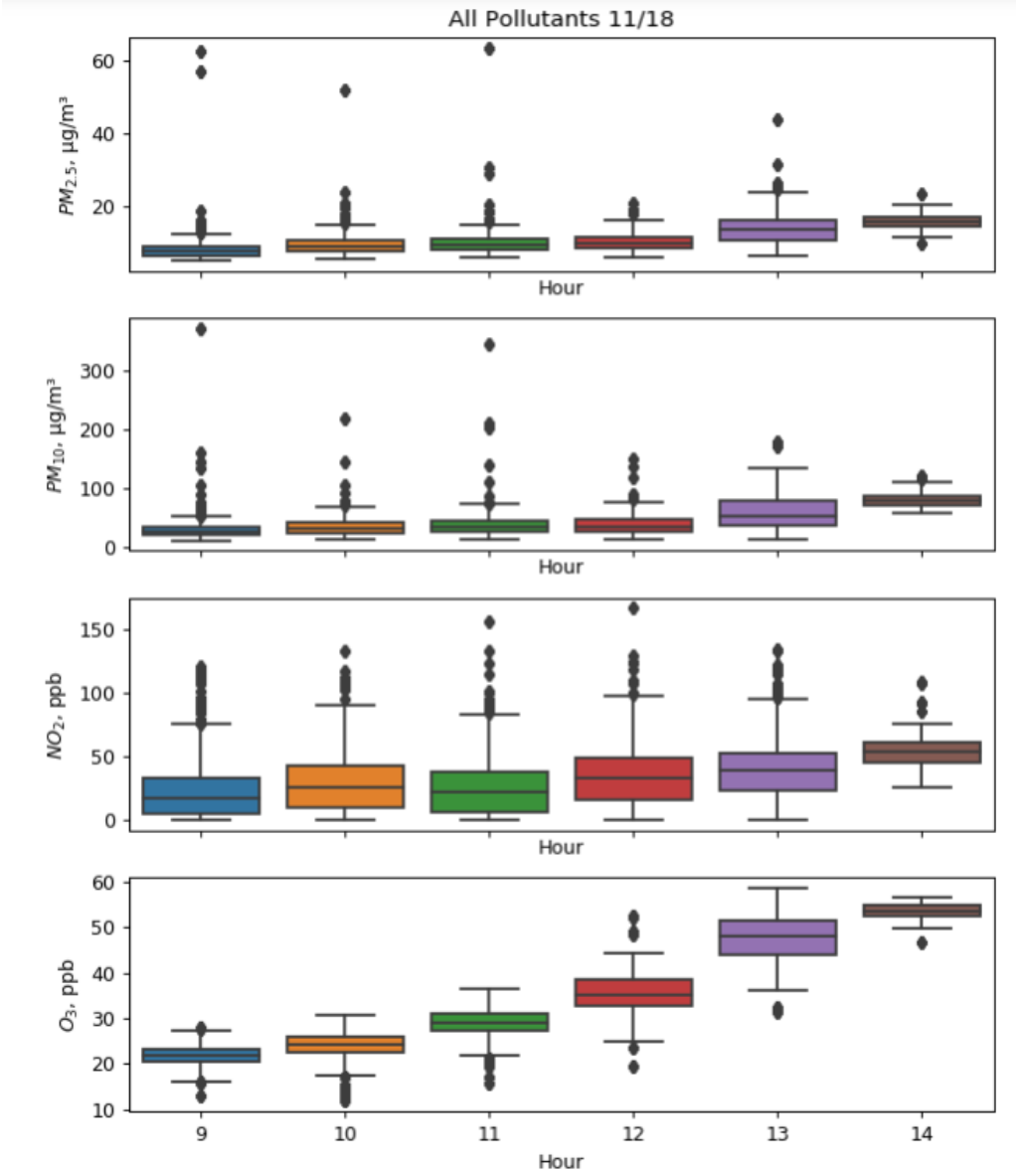

Figure B- 5 Hourly Boxplot: Pollutant Data For 11/18

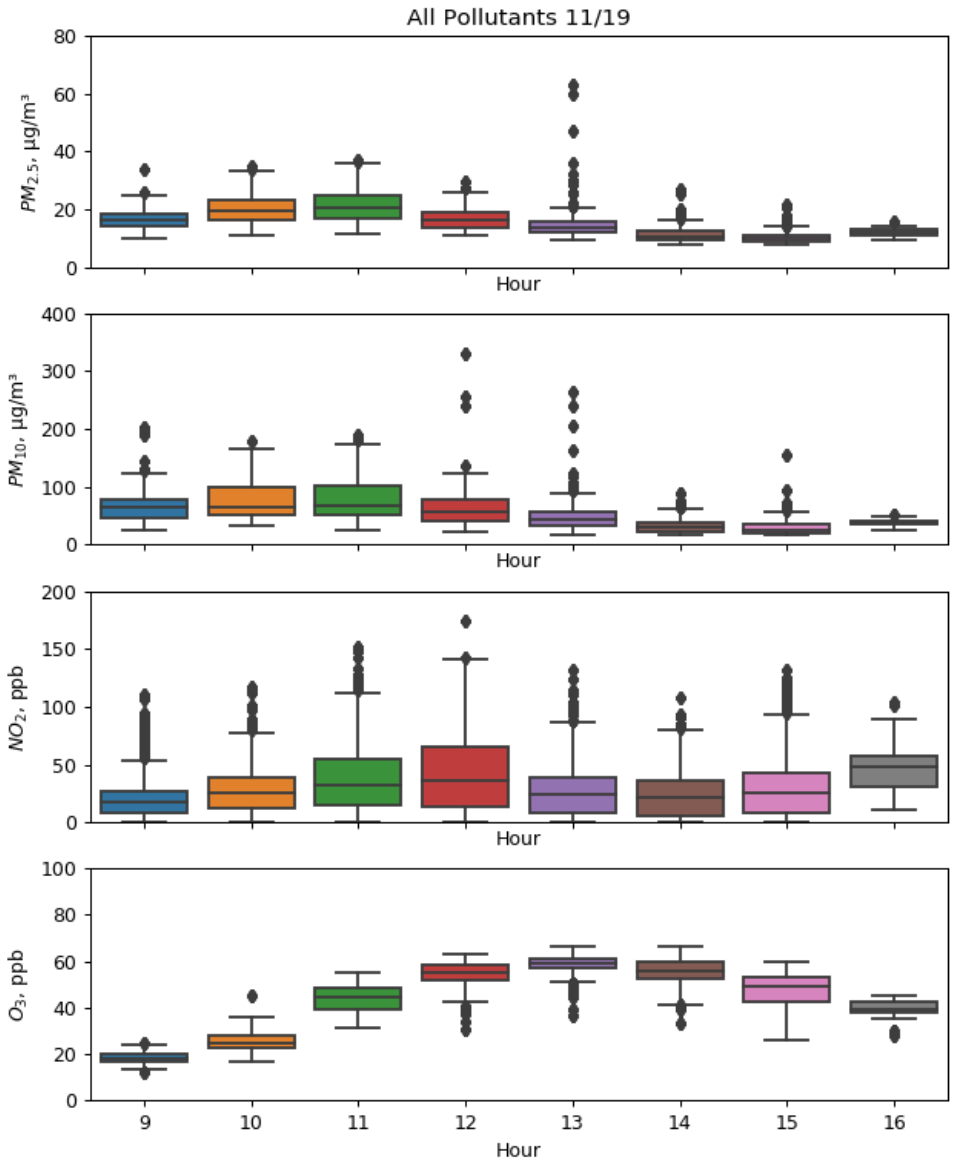

Figure B- 6 Hourly Boxplot: Pollutant Data For 11/19

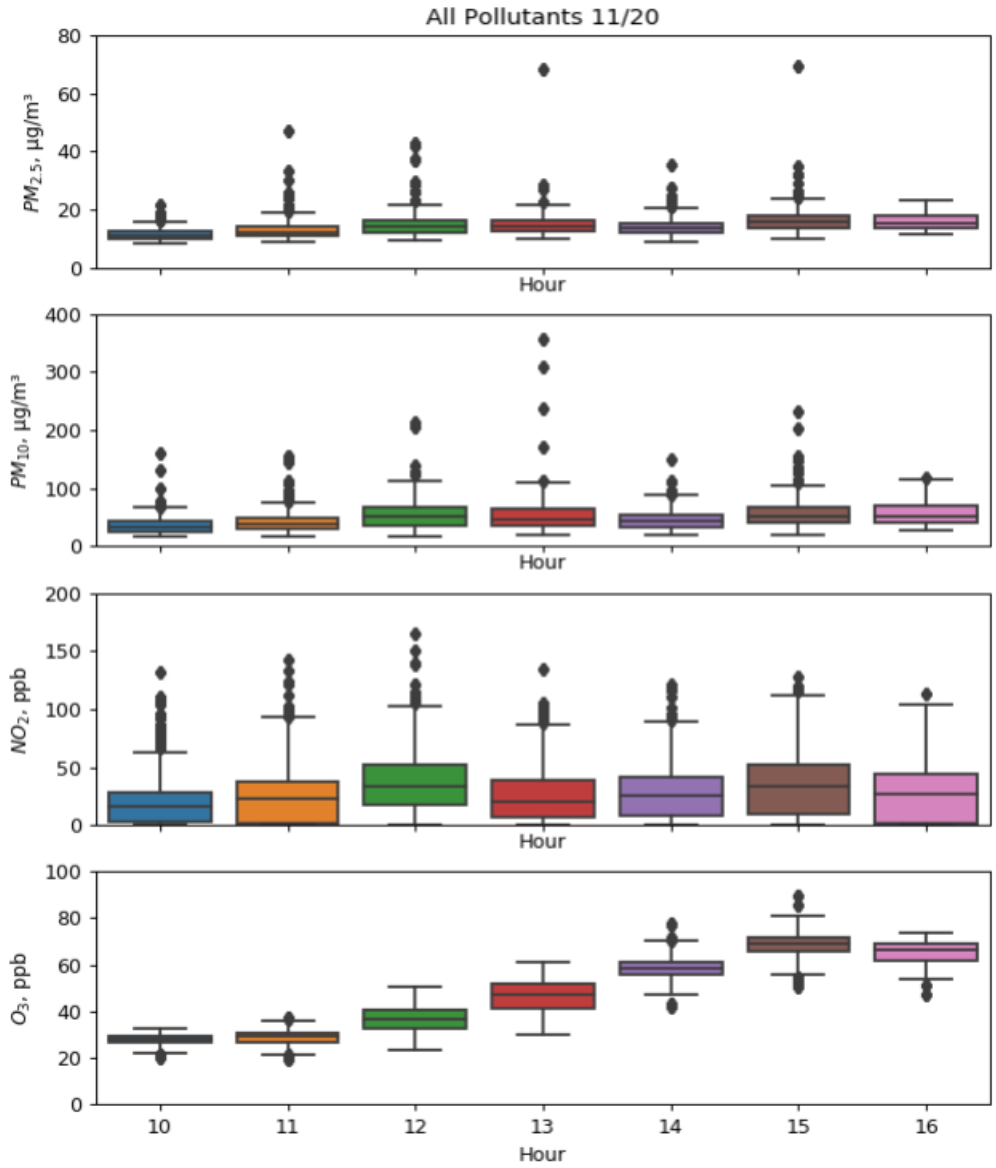

Figure B- 7 Hourly Boxplot: Pollutant Data For 11/20